

**ONTOGENY OF THE MU OPIOID RECEPTOR
IN THE FETAL RHESUS MONKEY BRAIN**

by

Josephine M. Moore

A DISSERTATION

Presented to the Department of Physiology & Pharmacology

and the Oregon Health Sciences University

School of Medicine

in partial fulfillment of

the requirements for the degree of

Doctor of Philosophy

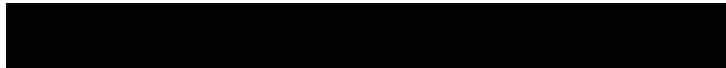
June 1997

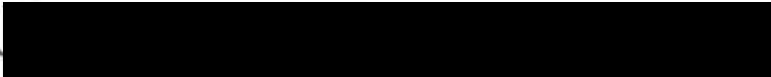
School of Medicine
Oregon Health Sciences University

CERTIFICATE OF APPROVAL

This is to certify that the Ph.D. thesis of
Josephine M. Moore
has been approved


Oline K. Ronnekleiv, Ph.D., Thesis Advisor


John A. Resko, Ph.D., Committee Chairman


Cynthia Bethea, Ph.D., Member


Elaine J. Lewis, Ph.D., Member

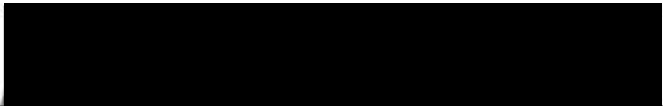

Richard A. Maurer, Ph.D.
Associate Dean for Graduate Studies

Table of Contents

Abstract.....	1
Introduction	2
Development of the Primate Brain	2
Review of Neurogenesis in the Brain	3
Mu Receptor Localization in the Brain and Spinal Cord	9
Physiological Actions of Mu Receptor	12
Antinociception	12
Cardiovascular and Respiration.....	13
Neuroendocrine Effects.....	14
Addiction	15
Neonatal Abstinence Syndrome	16
Morphine and β -Endorphin.....	16
Mu Receptor during Development	18
Molecular Characterization of the Mu Receptor	20
Mu Receptor mRNA in the Adult Rat	21
Materials and Methods.....	24
Animals	24
Tissue Preparation	24
Mu receptor cloning	24
RT PCR & Subcloning	
Transformation, Plasmid isolation, Sequence analysis	25
<i>in situ</i> Hybridization.....	26
Probe Preparation	
<i>in situ</i> Hybridization protocol.....	27
Autoradiography	
Control Experiments	
Analysis	
Binding Autoradiography.....	29
Tissue Treatment	
Specific and Non-specific Binding.....	29
Film Autoradiography	
Analysis	
Results.....	31
Fetal Growth	31
Morphological Maturation of the Fetal Monkey Brain.....	31
Day 40 and Day 45 fetal rhesus monkey	31
Day 60 fetal rhesus monkey	32
Day 70 fetal rhesus monkey.....	33
Day 130 and day 150 fetal rhesus monkeys.....	35
Mu Receptor mRNA in the Fetal Monkey Brain	35
Day 40 and 45 fetal rhesus monkeys.....	35
Day 60 fetal rhesus monkey.....	36
Day 70 fetal rhesus monkey.....	37
Day 130 fetal rhesus monkey thalamus.....	39
[³ H]-DAMGO Binding of Mu Receptor in the 70 and 150 Day Fetal Monkey	40
Mu Receptor mRNA and Mu Receptor Binding in the 70 Day Fetal Monkey	42
Discussion.....	45
Mu Receptor mRNA during Fetal Development	45
Mu Receptor Binding during Fetal Development	49
References.....	53
Figures & Tables	71

Acknowledgments

I would like to thank Dr. Oline Ronnekleiv for her guidance, expertise and professionalism throughout the preparation of this body of work. Thanks also goes to the other members of my committee, Drs. John Resko, Cynthia Bethea, and Elaine Lewis for the thoughtful and constructive criticism which made this project what it is. Special mention should and does go to Dr. John Resko for finding the funding that allowed me to stay in school and attain my goals. I would also like to thank Dr. Yuan Fang. Dr. Fang performed all of the binding experiments on the 70 day fetal monkeys and taught me all about the world of binding autoradiography. I would also like to thank Barry Naylor who taught me about in situ hybridization, cryostat sectioning, and dipping and developing slides. I cannot thank Martha Bosch enough for the time she has spent helping me get this together. She has shared in the ups and the downs and basically been my extended family while I have been in Portland.

I would like to dedicate this dissertation to my mother, Rose Poole Moore, and to the memory of my father, Joseph Stelzer Moore. I thank my sisters, Carolyn M. Cook and M'Liss R. Moore for their unerring support over the past two months. Finally, I would like to mention my grandmothers, Evelyn Cain Poole and Mary Stelzer Moore and my Portland family: Luci, Pup, Cleo, P.D., Ned, and Mouse. All have been my teachers in one way or another and all have been able to make me laugh. I couldn't have completed this without their positive reinforcement.

Abstract

The mu opioid receptor is the first of the opioid receptors to be expressed during development in the mammalian brain and has been implicated as a modulator of neuronal proliferation. Very little information, however, is known about mu receptor development in the fetal primate brain. The ontogeny of the mu opioid receptor was investigated in the fetal rhesus monkey at days 40, 45, 60, 70, 130, and 150 of an approximate 165 day gestation period. In situ hybridization for mu receptor mRNA was performed on cryostat sections using a 293 base pair rhesus monkey specific probe corresponding to transmembrane domains VI and VII of the human mu opioid receptor sequence. [3H]-DAMGO binding autoradiography was performed on cryostat sections in the days 70 and 150 fetal monkey. At days 40 and 45, mu receptor mRNA was found in the ventral thalamus, cerebellar plates and brainstem. By day 60, mu receptor mRNA expression was seen in the striatum, olfactory bulbs, septum, medial habenula, thalamus, and brain stem. At day 70, the striatal patches were apparent along with more extensive thalamic expression. In the 130 day fetus, mu receptor mRNA distribution in the thalamus was similar to the day 70 fetus but the cellular content was highly increased. In the day 70 fetal monkey brain, mu receptor binding sites corresponded well with the distribution of mu receptor mRNA. Mu receptor densities in the day 70 and day 150 fetal brain were also quite similar with the exception of the paraventricular nucleus of the thalamus and the arcuate nucleus of the hypothalamus which had much higher optical densities in the 150 day fetus. The mu receptor is expressed early in gestation in the fetal monkey brain and the distribution of the mu opioid receptor indicates that its presence in the developing limbic, sensory and motor systems of the fetal brain could actively participate in the modulation of the neural circuitry critical for survival after birth.

Introduction

Development of the Primate Brain

The development of the primate central nervous system begins with the formation of the neural plate which folds to form the neural groove and upon closure, the neural tube. The rostral aspects of the neural tube are destined to become the brain and the caudal aspects, the spinal cord. Brain development begins with two vesicular bulges. The rostral vesicle gives rise to the prosencephalon (forebrain) and the caudal vesicle forms the mesencephalon (midbrain) and the rhombencephalon (hindbrain). The forebrain and the hindbrain divide further to give a total of five vesicular regions which are, beginning rostrally: the telencephalon, diencephalon, mesencephalon, metencephalon and myelencephalon. The telencephalon gives rise to the cortex, olfactory bulbs, septum, hippocampus, amygdala, and striatum. The diencephalon forms the thalamus and hypothalamus. The mesencephalon develops into the midbrain. The metencephalon will become the pons and cerebellum. The most caudal structure, the myelencephalon, will be the medulla oblongata.

At the five vesicle stage, the lumen of this vesicular arrangement is the precursor of the ventricular system. The telencephalic vesicles surround the lateral ventricles; the diencephalon, the third ventricle; the mesencephalon, the aqueduct; and the metencephalon and myelencephalon, the fourth ventricle which continues into the spinal cord as the central canal. The neuroepithelium that lines the walls of the ventricles, contains the proliferative ventricular and subventricular zones which give rise to the migratory cells that eventually form the cortex and the nuclei of the brain (Lauder, 1995; Netter, 1986).

Review of Neurogenesis in the Brain

Formation of the neocortex in the rhesus monkey (*Macaca mulatta*) begins with the asynchronous division of cells in the proliferative zones lining the ventricular wall, a process which is completed by embryonic day 100 (E100) of a 165 day gestational period (Rakic, 1974; Rakic, 1988). These cells migrate along radial glial fibers that span the region between the ventricular and pial layers. They travel through the intermediate zone and form the cortical plate in an inside-out configuration (spatiotemporal arrangement). After the first postmitotic cells have migrated to the cortical plate, subsequently arriving cells migrate past their predecessors to form the more superficial layers of the neocortex (Rakic, 1974; Schmechel & Rakic, 1979; Sidman & Rakic, 1973). In the frontal association cortex, neurogenesis occurs between E47 and E90. Compared to other regions in the cortex, the migratory route in the frontal lobe is substantially longer (15 mm in the midgestational monkey). Although neurogenesis is complete around midgestation, the formation of cortical and subcortical connections is more protracted. Synaptogenesis begins between E47 and E78 and peaks between E130 and two months after birth. This peak in the development of synaptic connections is followed by a relatively stable period which lasts until puberty. From puberty through adulthood, there is a slow, steady decline in synaptic density (Rakic, 1995).

The olfactory bulb is another structure that is derived from the ventricular neuroepithelium in the rostral telencephalon. In the human, these structures begin to appear at day 44 of gestation (Bossy, 1980). In the monkey, the olfactory bulbs begin to develop and become distinct from the frontal lobe between 36 and 46 days of gestation (Gribnau & Geijsberts, 1981; Gribnau & Geijsberts, 1985). In the rat, putative receptor axons from the olfactory epithelium make contact with the telencephalon ventricular zone at E13 which results in the evagination of the olfactory bulb primordium on E14 (Gong & Shipley, 1995). In the main olfactory bulb, the neurogenesis of the mitral cells occurs between E15 and E16, ending on E18. The tufted cells are generated between E17 and E20. The

interneurons of the main bulb, which includes the periglomerular and granule cells, are all generated postnatally in the rat (Bayer, 1983).

The medial and lateral septal nuclei in the primate are derived from the neuroepithelium of the lateral ventricle which start to differentiate on E36. Peak neurogenesis occurs around E45 yet the cells continue to proliferate until E62. In contrast to the neocortex, the spatiotemporal gradient of the septum is outside-in. The cells that are generated first are closer to the pial surface (medial septum) than those which are generated later and located laterally or closer to the ventricular surface (lateral septum) (Brand & Rakic, 1980). It is interesting to note that the cholinergic neurons in the vertical limb of the diagonal band of Broca and in the nucleus basalis are born during the fifteen day period between E30 and E45 (Kordower & Rakic, 1990).

There is a large cell mass that bulges into the lateral ventricle, known as the ganglionic or ventricular eminence, which contains the progenitor cells that are predisposed to become, in part, the neostriatum (caudate, putamen, and nucleus accumbens) and amygdala (Figure A). The first cells destined for the neostriatum are born on E36 (Brand & Rakic, 1979). In the caudate and putamen primordium, there are two types of cells: the large neurons which represent the cholinergic interneurons and the small neurons that represent the numerous medium spiny projection neurons of the adult. The large cells are generated between E36 and E45 (Brand & Rakic, 1979). The small neurons are produced from E36 to E80; a time frame which correlates with the neurogenesis of the nucleus accumbens (E36-E86) (Brand & Rakic, 1980). In the adult primate striatum, the caudate and putamen are divided into two distinct compartments, the striosomes and the matrix. The striosomes contain a higher density of cells than the surrounding matrix and are patchy in appearance (Ilinsky & Kultas-Ilinsky, 1995; Kalil, 1978). During the birth of the neurons in the caudate and putamen, this clustering or patchy pattern is seen which indicates that the striosomes or patches are born first, a situation that is seen in the fetal rat (van der Kooy & Fishel, 1987). There is, however, no spatiotemporal arrangement during

the formation of the neostriatum in the monkey (Brand & Rakic, 1979; Brand & Rakic, 1980). The amygdala neurons are produced between E33 and E50 and do not display any

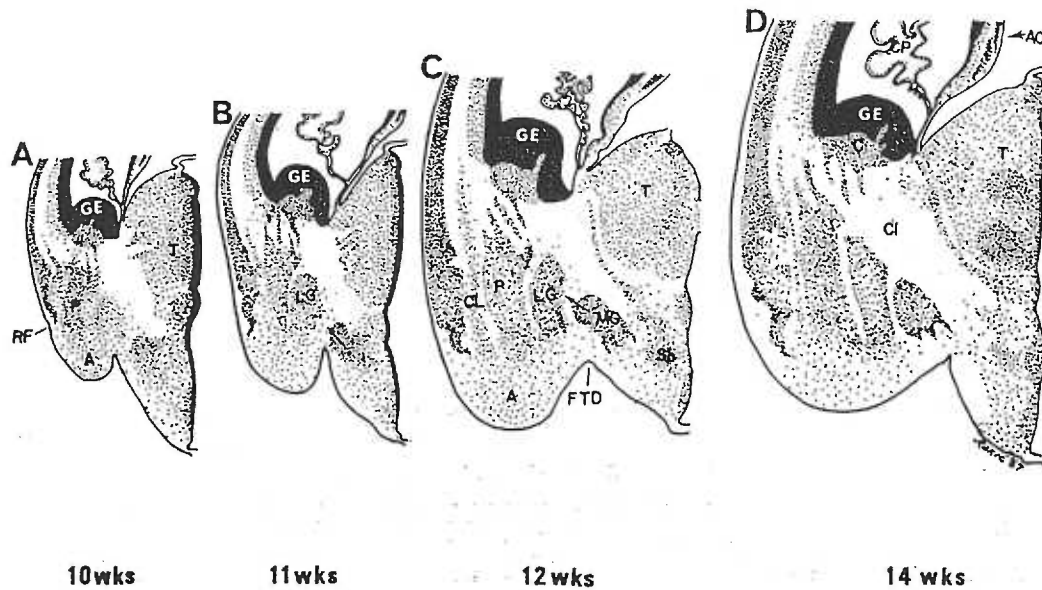


Figure A. Coronal sections at approximately the same level of the forebrain in 10- to 14-week human fetuses to illustrate the position of the ganglionic eminence (GE) a gradual shifting (arrow) of the medial segment of the globus pallidus (MG) from the diencephalon to the telencephalon across the tel-diencephalic fissure (FTD). Abbreviations: A, amygdala; AC, archicortex; C, caudate nucleus; CI, internal capsule; CL, claustrum; LG, lateral segment of the globus pallidus; P, putamen; RF, rhinal fissure; SB, subthalamic nucleus; T, thalamus.

Taken from Sidman and Rakic, 1973.

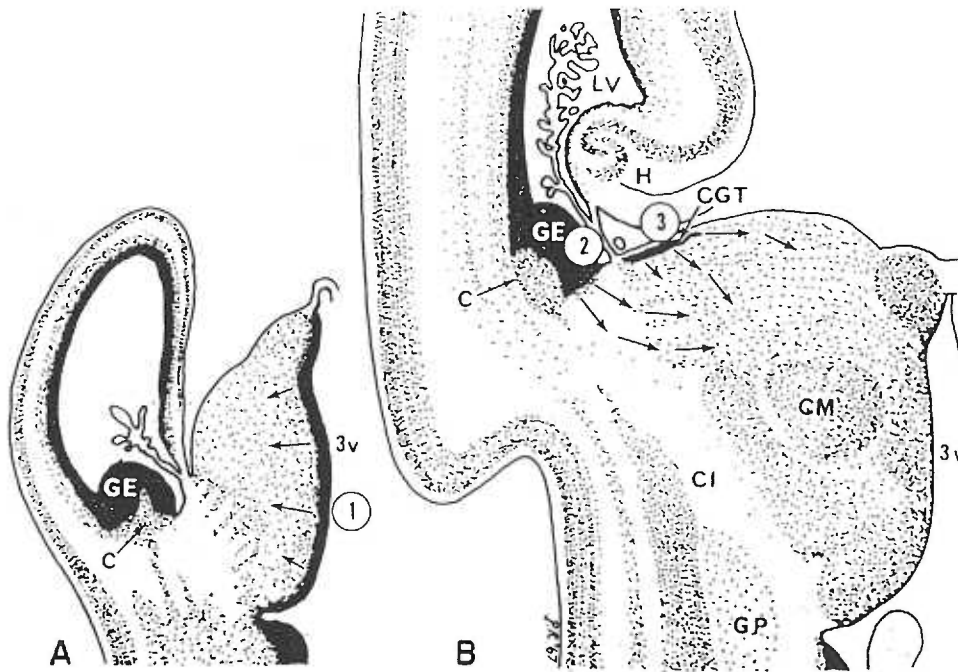


Figure B. Migration pathways to the posterior portion of the human thalamus. Semi diagrammatic drawings of the thalamus and adjacent structures sectioned in the horizontal plane. The arrows indicate the main paths of cell migration during formation of the thalamus. The left section is from a 10 week fetus and the right section is from a 24-week fetus. The arrows near the circled number 1 indicate that the ventricular zone in wall of the third ventricle serves as the source of thalamic neurons during early development. The arrows extending from the circled number 2 indicate the path of migration of cells from their origin in the ganglionic eminence (GE) across the incipient posterior thalamic peduncle and internal capsule to reach the lateral thalamus. The arrows at circled number 3 indicate another migration path that lies posterolaterally, the calls passing through the corpus gangliothalamicum (GCT) or gangliothalamic body into the thalamus. Migrations 2 and 3 come at a stage when the ventricular zone of the third ventricle is exhausted and yet the lateral and superior parts of the thalamus are expanding enormously. Abbreviations: C, caudate nucleus; CI, internal capsule; CM, nucleus centrum medianum; GP, globus pallidus; H, hippocampal formation; LV, lateral ventricle; 3V, third ventricle. Taken from Sidman and Rakic, 1973.

sort of gradient with respect to time of origin and migratory pattern (Kordower, et al., 1992).

The ventricular zone of the third ventricle and the ventricular or ganglionic eminence are the early sources of hypothalamic and thalamic neurons (Figure A, B). The neurogenesis of the primate hypothalamus begins on E27 in the supraoptic nucleus, the suprachiasmatic nucleus and the medial bed nucleus of the stria terminalis (van Eerdenburg & Rakic, 1994). This proliferation continues from E38 through E45 in most of the anterior hypothalamic nuclei. The cells which are generated last (E43-E48) are destined to become the medial preoptic area (van Eerdenburg & Rakic, 1994).

The thalamus is also derived from the neuroepithelium of the third ventricle until this source of neurons is exhausted (Sidman & Rakic, 1973). At this time, the ganglionic eminence is believed to supply cells which are distributed through the medially situated gangliothalamic body (Figure B). In the fetal human, it is thought that this structure gives rise to the pulvinar of the caudolateral thalamus (Sidman & Rakic, 1973). In the rat, the earliest thalamic structure to arise is the reticular nucleus (E13) whereas the rest of the thalamus is born between E14 and E18 (Altman & Bayer, 1988a).

In the mesencephalon and brainstem, the locus coeruleus is born between E27 and E36 in the fetal monkey with the medial cells generated earlier than those situated more laterally (Levitt & Rakic, 1982). The mesencephalic raphe nucleus is generated between E28 and E35 and the caudal raphe is born between E35 and E43. The raphe magnus neurons are generated between E38 and E40 (Levitt & Rakic, 1982). The substantia nigra neurons are born following the locus coeruleus and the mesencephalic raphe between E36 and E43 and do not exhibit a spatiotemporal gradient during their development nor can the pars compacta and the pars reticulata be distinguished at this stage (Levitt & Rakic, 1982).

A structure similar to the transient gangliothalamic body of the diencephalon is present in the human rhombencephalon (Figure C). This pontobulbar body is the source of

neurons which migrate mediolaterally to form the inferior olivary nucleus and the pontine gray (Sidman & Rakic, 1973). The adjacent rhombic lip gives rise to the external layer of the cerebellum. Both the pontobulbar body and the rhombic lip have contact with the fourth ventricle (Sidman & Rakic, 1973).

Mu Receptor Localization in the Brain and Spinal Cord

Non-Specific Ligands

In the early studies of opiate receptor binding in the primate brain, it was not yet known that subtypes of the opioid receptors existed so agonists or antagonists, which potentially bound all of the receptors were used. [³H]-Dihydromorphine, which is a relatively non-selective agonist yet has a slight propensity for mu receptor binding, was used to describe the regional distribution in primate brain homogenates (Kuhar, et al., 1973). The areas which displayed the most intense binding were the anterior amygdala and the periaqueductal gray. Moderate opioid receptor binding was seen in the hypothalamus, the medial thalamus, and the head of the caudate nucleus. Binding in the frontal cortex, hippocampus, putamen, superior colliculus and the interpeduncular nucleus were all approximately half of that seen in the hypothalamus and medial thalamus. [³H]-Dihydromorphine binding in human brain homogenates generally agreed with that seen in the monkey with the exception of the thalamus in which binding was as high as that seen in the amygdala. This contrasted to virtually no binding in the occipital lobe of the cortex and in the cerebellum in both species (Kuhar, et al., 1973). [³H]-Etorphine (a non-selective opioid agonist) binding in human brain homogenates agreed with but extended these findings (Hiller, et al., 1973). The septal nuclei, temporal lobe of the cortex and the pulvinar all had high opioid binding densities. The olfactory bulbs and the ventroanterior and ventroposterolateral nuclei of the thalamus displayed moderate opiate binding. There was also low binding in the occipital lobe of the cortex and the cerebellar cortex which

differed from the dihydromorphine binding studies but etorphine is a much less specific agonist and could have bound all three opioid receptors (Hiller, et al., 1973).

[³H]-Diprenorphine (a non-selective opioid antagonist) was used to assess the distribution of opiate receptors in cynomolgus monkeys (Wamsley, et al., 1982). In this study 500 µCi/kg body weight of tritiated diprenorphine was injected into the monkeys 1-1.5 hours before sacrifice after which, the brains were dissected and sectioned for autoradiography. The data from this study generally agreed with that previously described with the highest density of opioid binding in the amygdala, ventricular and intralaminar nuclei of the thalamus, hypothalamus, parabrachial nuclei, caudal spinal trigeminal nucleus, nucleus of the solitary tract, the marginal and gelatinosa layers of the spinal cord, and in the neurohypophysis. Moderate binding was apparent in the caudate and putamen, mediodorsal and centromedian and lateral nuclei of the thalamus, superior colliculus, ambiguus, dorsal motor nuclei, inferior olive and lamina III and IV of the spinal cord. The hippocampus, globus pallidus, reticular nucleus of the thalamus, substantia nigra pars compacta, and the ventral tegmental area were all shown to have low opiate receptor binding densities (Wamsley, et al., 1982). Due to the autoradiographic technique used in this experiment, a more precise localization of opiate receptor distribution was determined. The antagonist used however, was not able to distinguish between the opiate receptor subtypes due to the lack of specificity.

Specific Ligands

Naloxone is a well known opioid antagonist yet, depending on the concentration, it can be specific for the mu receptor. Concentrations of naloxone from 10⁻⁹ M to 10⁻⁸ M will preferentially bind to the mu receptor whereas micromolar concentrations will bind mu, kappa, and delta receptor sites (Goldstein & Naidu, 1989). D-Ala², N-Me-Phe⁴, Gly⁵-ol-Enk (DAMGO) is a mu specific ligand which binds to this receptor when used in concentrations from 10⁻⁹ M to 10⁻⁷ M, making it more specific for the mu receptor (Goldstein & Naidu, 1989; Handa, et al., 1981). In parasagittal and coronal sections of

adult rhesus monkey brain incubated with 1 nM [³H]-naloxone, distinct patches of naloxone binding were seen in the striatum and dense binding apparent in the amygdala and the bed nucleus of the stria terminalis. There was considerable mu binding in the hypothalamus, especially in the median eminence, arcuate, paraventricular nucleus and the supraoptic nucleus (Lewis, et al., 1984; Mansour, et al., 1988). Many of the thalamic nuclei had dense mu binding with particularly dense autoradiographic signal in the paraventricular nuclei. In the midbrain and brainstem, the interpeduncular nucleus, periaqueductal gray, nucleus of the solitary tract, and the spinal trigeminal nucleus all contain mu receptor binding sites (Lewis, et al., 1984). In most of these nuclei, POMC immunoreactivity is also evident with the exception of the bed nucleus of the stria terminalis, the amygdala and the interpeduncular nucleus which express enkephalin immunoreactivity. The medial preoptic area of the hypothalamus, the midline paraventricular nuclei of the thalamus, parabrachial, nucleus of the solitary tract and the spinal trigeminal nucleus also contain enkephalin as well as POMC immunoreactivity (Lewis, et al., 1984). Layers V and VI of the cerebral cortex contain high densities of mu receptor binding sites labeled with 2 nM naloxone. The auditory cortex and the inferotemporal cortex had the most mu receptor binding in layer V (Wise & Herkenham, 1982). In the monkey spinal cord, antibodies to the mu receptor were localized in lamina II with minor labeling seen in lamina I (Honda & Arvidsson, 1995).

Most of the areas which contain mu receptor in the primate also bind mu receptor in the rat (Delfs, et al., 1994b; Mansour, et al., 1995a; Mansour, et al., 1994; Mansour, et al., 1988). There are some species differences, however. The central nucleus of the amygdala is devoid of mu receptor binding in the rat yet the monkey has dense mu receptor binding in all amygdaloid regions (Lewis, et al., 1984; Mansour, et al., 1988). In the rat, the hypothalamus has virtually no binding in the supraoptic, paraventricular, arcuate, or ventromedial nuclei although low levels of mu binding are seen in the dorsomedial nucleus and the lateral hypothalamus (Mansour, et al., 1995a; Mansour, et al., 1988). As stated

above, the monkey brain contains high densities of mu receptor in the hypothalamus, specifically in the supraoptic nucleus, paraventricular nucleus, arcuate and the median eminence (Lewis, et al., 1984). The paraventricular nucleus of the thalamus is devoid of mu receptor binding in the rat whereas this region in the monkey contains dense mu binding sites (Lewis, et al., 1984; Mansour, et al., 1994; Mansour, et al., 1988).

Physiological Actions of Mu Receptor

Antinociception

The physiological actions of mu receptor activation are varied and many have been elucidated due to the effects of morphine administered to alleviate pain. Nociceptive fibers include both the unmyelinated C-fibers and the myelinated A δ -fibers. The former is associated with slow pain that is general in its localization and the latter with fast pain that has a more precise localization (Clifford, 1984). These primary afferent fibers enter the spinal cord through the dorsal horn. Secondary neurons traverse the spinal cord and ascend through the medulla and midbrain to the ventroposterolateral and intralaminar thalamus, on their way to the cortex via the lateral spinothalamic tract of the anterolateral funiculus (Clifford, 1984; Netter, 1986). Unilateral dorsal root rhizotomy in juvenile rhesus monkeys followed by in vitro receptor binding with naloxone (1 nM, a concentration which binds mu receptor (Goldstein & Naidu, 1989)) showed that transection of the ganglia reduced but did not abolish naloxone binding in the dorsal horn compared to the intact controls. This provided some of the first direct evidence that mu receptors were located on primary afferent neurons and in the neurons of the dorsal horn (Lamotte, et al., 1976). The presence of immunohistochemical proenkephalin found in the substantia gelatinosa (lamina II) of the spinal cord of the rat correlated well with this data (Mansour, et al., 1988). Administration of morphine directly to the spinal cord of the monkey was found to produce profound antinociceptive effects (Yaksh, 1983).

In the descending pain pathways, intraventricular morphine administration to the third ventricle or injection into the periaqueductal gray, raphe magnus, locus coeruleus, or the reticular formation will produce analgesia in rats which is reversible by naloxone administration (Fields, et al., 1991; Pasternak, 1993). It should be noted that enkephalin immunoreactivity is apparent in all of these areas in both the monkey and the rat (Lewis, et al., 1984; Mansour, et al., 1988). The periaqueductal gray excites neurons in the rostroventral medulla (including the raphe magnus and the reticular formation) which in turn project to the spinal trigeminal nucleus and spinal cord and inhibit nociceptive stimuli by releasing serotonin. Morphine injection into the reticular formation stimulates at least some of these serotonin releasing cells (Fields, et al., 1991). Combined immunocytochemistry and retrograde tracing techniques have located mu receptor containing cells in the periaqueductal gray that project to the rostroventral medulla. The rostroventral medulla, which in turn projects to the spinal cord, also contains cells which contain mu receptor immunoreactivity (Kalyuzhny, et al., 1996).

Cardiovascular and Respiration

Morphine and β -endorphin administration can result in cardiovascular and respiratory depression. In hypovolemic baboons, cardiac output decreased as endogenous β -endorphin increased. Naloxone administration during the hypovolemic state produced decreases in heart rate and increases in cardiac output and mean arterial pressure (McIntosh, et al., 1986). In adult monkeys, exogenously administered morphine (0.15 and 0.60 mg/kg) and β -endorphin (0.7 and 2.8 mg/kg) initially produce an increase in heart rate and blood pressure followed by a decrease in both parameters. The duration of these effects differed however, in that β -endorphin had a transient effect and morphine depressed the system throughout the entire experimental period of 150 minutes (Cuthbert, et al., 1989). β -endorphin did not have an effect on respiration although the analgesic dose of morphine (0.60 mg/kg) resulted in hypoventilation (Cuthbert, et al., 1989). Morphine is thought to depress respiration by reducing the sensitivity to carbon dioxide at the central and

peripheral chemosensory areas. The carotid and aortic bodies convey impulses to the nucleus of the solitary tract in the medulla via the glossopharyngeal and vagus nerves. These cranial nerves were shown to bind diprenorphine (Atweh & Kuhar, 1977). The nucleus of the solitary tract contains proenkephalin and proopioidmelanocortin as evidenced by immunohistochemical staining and in situ hybridization (Lewis, et al., 1984; Mansour, et al., 1988). In apneic fetal sheep, naloxone increases sensitivity to carbon dioxide (administered to the dam) by initiating sustained breathing movements (Moss & Scarpelli, 1979). In full term human fetuses, β -endorphin is three times higher than adult levels and has been shown to be released in response to hypoxia (Wardlaw, et al., 1979). Agonist activation of the mu receptor may also affect respiratory rhythmicity at the parabrachial nucleus and the ventrolateral medulla, areas which bind naloxone (at concentrations specific for mu receptor) in the human infant (Kinney, et al., 1990).

Neuroendocrine Effects

β -endorphin has also been shown to modulate the hypothalamic-pituitary-gonadal axis in monkeys and rats. The pulsatile release of gonadotropin releasing hormone (GnRH) from the hypothalamus results in the release of the gonadotropins from the pituitary which govern steroidogenesis and gametogenesis in the gonads. During the follicular phase, the pulsatile rate of luteinizing hormone (LH) is approximately once an hour whereas in the luteal phase, the pulses are decreased to one every three to ten hours. The pulsatility of LH is dictated by the GnRH pulse generator. β -endorphin has been shown to decrease gonadotropin secretion by acting either directly or indirectly on GnRH neurons (Chen, et al., 1989; Ferin, 1993). During menstruation in monkeys, plasma steroids and β -endorphin are all minimal, a condition also seen after ovariectomy. During the remainder of the menstrual cycle, serum β -endorphin increases as the steroids increase, reaching a peak during the luteal phase, in the presence of progesterone (Ferin, 1989). Push pull perfusion in monkeys given the mu opioid antagonist nalmefene did not affect GnRH secretion during the follicular phase compared to intact, untreated controls, although

mu antagonism increased GnRH secretion during the luteal phase when progesterone is highest (Pau, et al., 1996). The inhibition of GnRH secretion by β -endorphin seems to be related to the amount of steroids present. Estrogen has been shown to reduce the sensitivity of hypothalamic neurons to endogenous opioids in the guinea pig (Kelly, et al., 1992). In the presence of progesterone, or the reduction of estrogen concentration, β -endorphin acting at the mu receptor inhibits GnRH pulses and gonadotropin release (Ferin, 1989; Ferin, 1993; Pau, et al., 1996).

Morphine has also been shown to increase prolactin and growth hormone release in the rat (Pechnick, et al., 1985; Pfeiffer & Herz, 1984). Growth hormone release is probably due to the suppression of somatostatin but an effect on growth hormone releasing hormone can not be ruled out (Pechnick, et al., 1985). Prolactin release is inhibited by dopamine and it is thought that opioids inhibit these dopaminergic neurons to increase prolactin secretion. Subcutaneous administration of sufentamil, a mu selective agonist stimulates prolactin secretion in immature (5, 10, 15, and 20 days of age) and adult rats. The mu antagonist β -funaltrexamine blocks this response (Blackford, et al., 1992).

Addiction

Acute opiate exposure which inhibits adenylyl cyclase results in a decrease in cAMP and therefore a decrease in protein phosphorylation by protein kinase A (Childers, 1991). Prolonged exposure to opiates results in the development of tolerance, a state in which neuronal inhibition is overcome, adenylyl cyclase activity slowly increases, and firing rates return to the pre-opiate state (Childers, 1991; Harris & Nestler, 1993). Chronic opiate exposure will eventually result in dependence and an increase in adenylyl cyclase and protein kinase A. There is also an increase in the Gi and Go alpha subunits but this is accompanied by a reduction in their functional activity, presumably due to the uncoupling of the G-proteins and the receptor (Nestler, 1996). This upregulation of the G-protein/cAMP system also results in an increased set point for neuronal activation, a condition known as tolerance (Harris & Nestler, 1993). Removal of the opiates or the

administration of opioid antagonists will result in withdrawal due to the removal of the inhibitory action of the opioids and a rebound increase in adenylyl cyclase activity (Harris & Nestler, 1993).

Neonatal Abstinence Syndrome

There are approximately 3.5 million people in the United States that are classified as opioid addicts, many of whom are female and of child-bearing age (Foley, 1993). It has been estimated that 75,000 children born each year in the US are exposed to opiates during gestation. Many of these infants suffer from neonatal abstinence syndrome, a condition where the infants have become addicted to the opiate(s) taken by the mother during pregnancy, and suffer withdrawal symptoms after delivery. These symptoms include irritability, tremor, gastrointestinal dysfunction, and respiratory distress (Chiriboga, 1993; Franck & Vilardi, 1995). This condition lasts an average of 21 days after birth and usually requires hospitalization (Franck & Vilardi, 1995). The long term effects on development are not yet known although increased activity, attention deficit, and neuromotor disturbances are seen in children one to three years of age (Chiriboga, 1993).

Morphine and β -Endorphin

Morphine is the natural ligand for the mu receptor and the substance from whence the receptor got its name, based on behavioral and physiological evidence (Martin, et al., 1976). Although morphine has been used as an analgesic and anti-anxiety agent since its isolation from opium poppy sap in 1803, its mode of action was not known. That animals, including humans, possessed an endogenous receptor which responded to the plant alkaloid was first realized in 1973 with the discovery of specific receptor sites sensitive to morphine in nervous tissue (Kuhar, et al., 1973; Pert & Snyder, 1973; Simon, et al., 1973; Terenius, 1973). It was later discovered that human and rat cerebrospinal fluid contained a peptide which inhibited the binding of dihydromorphine in bioassays (Terenius & Wahlstrom, 1974). The peptide(s) turned out to be the endogenous opioid peptides met-

and leu-enkephalin ("in the head") which were isolated from porcine brain (Hughes, et al., 1975). β -endorphin ("endogenous morphine") was isolated in 1976 (Li & Chung, 1976) and found to be more potent, on a molar basis, than morphine as an analgesic and later, as the most potent endogenous ligand for mu receptor (Loh, et al., 1976; Schoffelmeer, et al., 1991). Proopiomelanocortin (POMC) is the large precursor protein from which β -endorphin, adrenocorticotropin, and melanocyte stimulating hormone are derived. The nucleotide sequence of POMC was published in 1979 (Nakanishi, et al., 1979; Roberts, et al., 1979) along with protein characterization studies which indicated that β -endorphin 1-31 (or β -LPH 61-91 in the older literature) was the biologically active opioid and that N-acetylation of this molecule rendered it inactive (Smyth, et al., 1979). POMC mRNA was localized to the cells of the arcuate nucleus of the hypothalamus and the anterior and intermediate lobes of the adult rat pituitary using in situ hybridization and solution hybridization with cDNA probes (Civelli, et al., 1982; Gee, et al., 1983).

Immunocytochemistry coupled with tritiated thymidine injection in fetal rats indicated that the POMC cells of the arcuate nucleus first appear on E12 (Khachaturian, et al., 1985). Although no studies have been performed in the fetal monkey, the adult rhesus contains POMC immunoreactive cells in the arcuate nucleus which project rostrally to innervate the nucleus accumbens, the diagonal band of Broca, the septum and the bed nucleus of the stria terminalis (Khachaturian, et al., 1984). POMC cell fibers are dense in the monkey hypothalamus including the medial preoptic area, anterior hypothalamus, peri- and paraventricular nuclei, dorsal medial hypothalamus and the median eminence. The lateral projections from the arcuate nucleus innervate the medial basal hypothalamus and the medial and central amygdala. Caudally, the arcuate POMC cells project to the periaqueductal gray, the ventral tegmental area, the superior and inferior colliculi and the parabrachial nucleus. Immunoreactive POMC fiber tracts are not apparent in the medulla but fibers are seen in the dorsal raphe, raphe magnus, sensory and motor nuclei of the spinal trigeminal, the ambiguus, and the nucleus of the solitary tract (Khachaturian, et al.,

1984). Immunoreactive POMC containing cells are found in the nucleus of the solitary tract of rats but not in the monkey (Khachaturian, et al., 1984). POMC immunoreactivity in the rat corresponds well with that seen in the monkey with a few exceptions. The rat caudate-putamen does not contain immunoreactive POMC but the monkey contains fibers in the head of the caudate and putamen (Khachaturian, et al., 1984). In the septum, the monkey has but a few POMC fibers present with the rat having more immunoreactivity in this region. In the amygdala, the monkey contains POMC fibers which are localized in the medial and central nuclei. The rat has POMC fibers in all of the amygdala nuclei (Khachaturian, et al., 1984).

Mu Receptor during Development

In the fetal mouse, the endogenous opioid peptides (β -endorphin, met-enkephalin and dynorphin) are all present by day E11.5 with β -endorphin immunoreactivity being two to three fold higher than that of enkephalin or dynorphin (Elkabes, et al., 1989; Rius, et al., 1991). Also in the mouse, mu receptor is the first of the opioid receptors expressed during development (E12.5) with the kappa opioid receptor being expressed at E14.5. The delta opioid receptor is not detected during the fetal period in the mouse (Rius, et al., 1991). In the fetal rat, preproenkephalin mRNA was detected by E15 in the proliferative layers of the neuroepithelium (Zagon, et al., 1994). Prodynorphin mRNA is detected in the developing ventromedial hypothalamus and the striatum at E16 of fetal rat development and in the supraoptic nucleus of the hypothalamus and in the hippocampus by E18 (Laurent-Huck, et al., 1993). Dynorphin binds preferentially to the kappa receptor and β -endorphin to the mu receptor. Enkephalin, however, will bind to both the mu and the delta opioid receptors but since the delta receptor has not been found during fetal development enkephalin may be binding to the mu receptor.

There has only been one developmental study done in primate, to our knowledge, which utilized tritiated naloxone at concentrations specific for mu receptor in the fetal (19-

21 weeks of gestation) and infant (6-38 postnatal weeks) human brainstem (Kinney, et al., 1990). In the fetuses studied, mu receptor binding was present in the midbrain interpeduncular nucleus, periaqueductal gray and the cuneiform nucleus. In the pons, there was considerable mu binding in the parabrachial and locus coeruleus. In the medulla, the inferior olivary nucleus, spinal trigeminal nucleus, nucleus of the solitary tract, ventral cochlear and hypoglossal nucleus all had dense mu receptor binding. The spinal cord had mu binding sites in lamina II. The most intense binding was seen in the interpeduncular nucleus and the inferior olivary nucleus. This same pattern was seen in the infant although moderate binding was also apparent in the dorsal raphe, raphe pontis, raphe magnus, lateral lemniscus, and nucleus ambiguus. Naloxone binding autoradiography (1 nM, which is specific for mu receptor) in coronal or sagittal sections of fetal rat brain demonstrated that the mu receptor is present in the fetal striatum, including label in the neuroepithelial layers, at E14 and in the accumbens, septal region, pallidum, and the olfactory cortex at E16 (Edley & Herkenham, 1984; Kent, et al., 1982). The striatum does not achieve the adult patchy distribution of mu receptor binding until at least week two of postnatal development (Edley & Herkenham, 1984; Kent, et al., 1982).

Neurogenesis in the primate central nervous system is completed during the first half of gestation with the exception of the cortex which continues just beyond that time point (Rakic, 1974; Rakic, 1988). In the rat, which has an gestation period of 22 days, neurogenesis takes place during the second half of gestation and into the postnatal period in some instances. There is now evidence that the cells which comprise the proliferative zones of the ventricles express receptors for stimulatory neurotransmitters that promote proliferation including the serotonergic 5HT-1 and dopaminergic D1 receptors, among others (Lidow & Rakic, 1995). In the postnatal rat, endogenous opioid peptides and opioid antagonists also affect cellular genesis. When rat pups are given doses of the non-selective opioid antagonist, naltrexone, that occupy opioid receptors for twelve hours or less, brain and body weights are reduced. However, rat pups given doses of naltrexone

which effectively blocked opioid receptors for twenty four hours were shown to have increases in brain and body weight (Zagon & McLaughlin, 1984). The effects of opioids were further studied by determining cell proliferation by the number of cells incorporating [³H]-thymidine. Six day old pups were given naltrexone at doses which block opiate receptors either continuously for 24 hours or transiently for less than 12 hours followed by intraperitoneal injections of [³H]-thymidine. Opioid receptor blockade increased cell proliferation in the cerebellar external germinal layer. In rat pups given met-enkephalin, the number of cells which incorporated [³H]-thymidine were reduced (Zagon & McLaughlin, 1987). In addition, continuous opiate receptor blockade (≥ 24 hours) has been shown to increase dendritic and neuronal spine diversification in pyramidal cells of the cerebral cortex and the CA1 field of the hippocampus and cerebellar Purkinje cells (Hauser, et al., 1989). In the human fetus born to heroin addicted or methadone treated mothers, there is a reduction in head size, body weight, and organ development (Chiriboga, 1993). The opioid receptors could therefore participate in the regulation of brain as well as general development.

Molecular Characterization of the Mu Receptor

It was not until the cloning of the rat mu opioid receptor in the early nineties that the DNA structure was identified (Bunzow, et al., 1995; Chen, et al., 1993; Kraus, et al., 1995; Thompson, et al., 1993; Wang, et al., 1993). It was then possible to locate the cells which synthesize mu receptor using in situ hybridization and compare this to binding autoradiography data of the receptor sites.

The mu opioid receptor is a protein consisting of 398-400 amino acids that has seven membrane spanning alpha helices of 17-25 amino acids each, an extracellular amino terminus and an intracellular carboxyl terminus, all of which are typical of G-protein coupled receptors (Birnbaumer, et al., 1990; Mestak, et al., 1995; Thompson, et al., 1993; Wang, et al., 1993). The rat and human mu receptor contain five N-linked glycosylation

sites and phosphorylation sites for protein kinase A, protein kinase C and calcium calmodulin kinase II (Mestak, et al., 1995; Thompson, et al., 1993). There are two transcriptional start sites in the promoter regions of the rat gene as well as potential sites for the AP-1 transcription factor (Kraus, et al., 1995). Agonist binding to the mu receptor modulates neuronal activation states through pertussis toxin sensitive G-proteins by inhibiting adenylyl cyclase and voltage dependent calcium channels as well as activating an inward rectifying potassium channel (Duman, et al., 1988; Loose & Kelly, 1990; Mestak, et al., 1995; North, et al., 1987; Seward, et al., 1991).

Mu Receptor mRNA in the Adult Rat

The paucity of information on mu receptor mRNA in the monkey is sharply contrasted with that for the rat. In most instances, mu receptor binding, using the mu specific ligand DAMGO, correlates well with mu receptor mRNA localization in the rat. Binding sites are seen in all layers of the olfactory bulb with a slightly more dense pattern seen in the external plexiform layer. Mu receptor mRNA is evident in the internal granular layer, mitral cell layer, and glomerular layer (Mansour, et al., 1994). In the cortex, the frontal lobe contains an abundance of mu receptor binding but little mRNA (Delfs, et al., 1994a; Mansour, et al., 1995a; Mansour, et al., 1994). In the striatum, the accumbens and the septum there is good correspondence between mu receptor binding sites and mRNA expression. Mu receptor binding, mRNA and immunoreactivity are all localized within the striatal patches and along the border of the striatum and the corpus callosum known as the subcallosal streak. Mu receptor binding and mRNA have a more intense concentration of patchy distribution in the rostral and lateral regions of the striatum (Mansour, et al., 1994). In the septum, both mu receptor binding and mRNA are found in higher concentrations in the medial versus the lateral nuclei. There is also a moderate amount of mu binding density and mu receptor mRNA label in the diagonal band of Broca. In the hippocampus, mu receptor binding and mu mRNA are located in the pyramidal layers of CA1-CA3, an area

which also displays mu receptor immunoreactivity. The other cell layers which include the strata oriens and radiatum contain little binding activity (Arvidsson, et al., 1995; Delfs, et al., 1994a; Mansour, et al., 1994). In the central nucleus of the amygdala, there is a modicum of mu receptor mRNA but virtually no mu receptor binding (Delfs, et al., 1994a; Mansour, et al., 1994).

In the thalamus of the adult rat, the anterior nuclear group and the reticular nucleus do not display mu receptor binding or mu receptor mRNA. The paraventricular nucleus has mu receptor mRNA but no mu receptor binding. The other nuclei of the thalamus including the mediodorsal, rhomboid and reuniens, centromedial, centrolateral, laterodorsal, lateroposterior, and medial and lateral geniculate nuclei have both mu receptor binding and mu receptor mRNA. In the epithalamus, the medial habenula contains mu receptor binding and mu receptor mRNA yet the lateral habenula is devoid of both. The hypothalamic nuclei which contain mu receptor mRNA include the medial preoptic area, arcuate, dorsomedial nucleus, lateral hypothalamus and medial mammillary nuclei. Each of these areas also show very slight mu receptor binding with the exception of the medial mammillary bodies which contain dense mu receptor binding (Delfs, et al., 1994a; Mansour, et al., 1995a; Mansour, et al., 1994). The superior colliculus consists of three layers: the superficial gray, the intermediate gray and the deep gray. Moderate mu receptor binding densities along with mu receptor mRNA are contained in the latter two whereas, the superficial gray, while devoid of mu receptor mRNA, displays abundant mu receptor binding sites in the adult rat. The inferior colliculus contains both mRNA and binding sites for the mu receptor. The substantia nigra (pars compacta and pars reticulata) and the ventral tegmental area all have mu receptor binding sites but only the pars compacta of the substantia nigra and the ventral tegmental area contain moderate amounts of mu receptor mRNA (Delfs, et al., 1994a; Mansour, et al., 1995a; Mansour, et al., 1994). The interpeduncular nucleus contains a dense concentration of mu receptor binding sites and mu receptor mRNA (Delfs, et al., 1994a; Mansour, et al., 1995a; Mansour, et al., 1994). The

locus coeruleus and the parabrachial nucleus contain dense mu receptor binding sites which correlate with the mu receptor mRNA as do the nucleus ambiguus, median raphe, the nucleus of the solitary tract and the spinal trigeminal nucleus (Delfs, et al., 1994a; Mansour, et al., 1995a; Mansour, et al., 1994). The cochlear nucleus contains high levels of mu receptor binding but relatively little mu receptor mRNA (Mansour, et al., 1994). The reticular formation shows relatively low levels of both mu receptor binding and mu receptor mRNA (Delfs, et al., 1994a; Mansour, et al., 1995a; Mansour, et al., 1994). The inferior olivary nucleus and the cerebellum do not exhibit mu receptor binding in the rat, although the medial cerebellar nucleus and the interposed nucleus contain cells which express mu receptor mRNA (Mansour, et al., 1995a; Mansour, et al., 1994). In the spinal cord, laminae I and II display the highest mu receptor binding yet mu receptor mRNA is more abundant in laminae V and VII (Arvidsson, et al., 1995; Mansour, et al., 1994). The dorsal root ganglia contains a conspicuous amount of mu receptor mRNA and mu receptor immunoreactivity (Arvidsson, et al., 1995; Mansour, et al., 1995a; Mansour, et al., 1995b; Mansour, et al., 1994).

The endogenous opioid peptides are detected early in fetal development in the rat and mouse. The mu opioid receptor, which binds β -endorphin and enkephalin, is the first of the opioid receptors to be expressed and is followed by the expression of the kappa opioid receptor which binds dynorphin. The delta receptor, which has a preference for enkephalin, appears not to be expressed during fetal development in the mouse. The opioid receptors have also been shown to modulate neuronal proliferation. In light of the fact that morphine, heroin and methadone bind to the mu opioid receptor, which is expressed early in development and that the mu receptor may have an effect on neurogenesis, plus the lack of information concerning mu opioid receptor development in the fetal monkey, the ontogeny of the mu receptor in the fetal monkey brain was investigated.

Materials and Methods

Animals

Animal care and use were in accordance with our institutional guidelines based on NIH standards. Adult female rhesus monkeys (*Macacca mulatta*) were paired with fertile males for three days between day nine through day eighteen of their menstrual cycle, based on an analysis of their previous menstrual cycle lengths. Pregnancy was determined by RIA analysis of estrogen (>100 pg/ml) and progesterone (>2.5 ng/ml) in blood samples obtained twenty to twenty-two days after pairing (Hess, Spies, & Hendricks, 1981). The second day of pairing was chosen as the day of conception from which gestation times were calculated. The fetuses were delivered by Cesarean section at days 40, 45, 60, 70, 130, and 150 of gestation.

Tissue Preparation

Body weight, crown rump length, and head circumference were recorded (Table I). The brains were then removed, dissected and fixed by immersion in ice cold 4% paraformaldehyde in 67 mM Sorensen's buffer, pH 7.2, except for the day 40 fetuses, in which the whole head was submerged. Fixation times varied from four to six hours depending on the size of the brain. Following fixation, the brains were soaked in 20% sucrose in 0.1 M sodium phosphate buffer (pH 7.2) overnight at 4°C. All solutions were prepared using molecular biology grade RNase free reagents and diethyl pyrocarbonate-treated water to insure an RNase free environment. Brains were then infiltrated with O.C.T. embedding media (Miles Laboratories), placed in Tissue-Tek cryomolds, frozen in liquid isopentane chilled to -55°C on dry ice, and stored in liquid nitrogen. The brains were sectioned coronally at 15 µm on a Leica cryostat, thaw mounted on to positively charged microscope slides (Fisher Brand) and stored at -80°C.

Mu receptor cloning

RT PCR & Subcloning: A fragment of the rhesus monkey mu receptor gene was cloned using reverse transcription polymerase chain reaction (RT-PCR) (Chai et al, manuscript in

preparation). Two oligonucleotide primers were designed from the human mu receptor sequence which corresponded to the coding sequence between transmembrane (TM) VI and TM VII (5'-primer: 831-CTTCGAAGGATCACCAGGAT-850; 3'-primer: 1105-ATTCGTCAGAACACTAGAGA-1124). The cDNA fragment was amplified using monkey thalamus total RNA (TRIZOL, Life Technologies, Inc.) with murine Moloney leukemia virus reverse transcriptase and AmpliTaq® polymerase (Gene Amp RT-PCR; Perkin-Elmer). First strand synthesis was achieved using 42°C for 15 minutes, 99°C for 5 minutes, 5°C for 5 minutes after which PCR followed for 40 cycles at 92°C for 30 seconds (denaturation), 53°C for 30 seconds (annealing), and 72°C for 45 seconds (elongation). The resulting 293 base pair PCR product was purified on a 3% agarose gel. The purified fragment was subcloned into the pGEM®-T vector (Promega) using 293 ng PCR product, 100 ng pGEM®-T vector, and 4 U T4 DNA ligase. The ligation proceeded overnight at 16°C.

Transformation, Plasmid isolation, Sequence analysis: The ligation reaction was transformed into the ampicillin resistant Escherichia coli strain XL-1 Blue subcloning grade competent cells as described by the manufacturer (Stratagene). Briefly, the cells were thawed on ice and 50 µl of the competent cells were aliquoted into Falcon 2059 tubes. β-mercaptoethanol was added (.85µl of 1.42 M) to increase the transformation efficiency. 50 ng of ligation mixture was added to the competent cells and incubated on ice for 30 minutes. The cells were heat shocked by placing the tubes in a 42°C water bath for 45 seconds and then incubated on ice for 2 minutes. Luria Broth (LB: 1% Bacto-tryptone, 1% NaCl; 0.5% Bacto-yeast extract, pH 7.4) medium containing 100 µg/ml of ampicillin was added and the cells were grown in a shaking incubator at 37°C for 1 hour. The transformed cells (100 µl) were spread onto LB-ampicillin agar plates, to which IPTG and X-Gal had been added. The plates were placed in a 37°C incubator overnight. Positive colonies were transferred to 5 ml of LB medium (100µg/ml ampicillin) and grown overnight in a shaking incubator (225-250 rpm) at 37°C. The cells were separated from the medium by

centrifugation and lysed. The plasmid was isolated from this mini-preparation and analyzed for size on a 1.5% agarose gel. The plasmids which were approximately 3.3 kb in size were characterized further by restriction endonuclease analysis. The plasmid (5 µg) was cut with 10 U of Nco I at 37°C for one hour. The cut plasmid was phenol/chloroform extracted to remove proteins and then precipitated in 100% ethanol. It was then cut with 10 U Pst I at 37°C for one hour, run on a 3% agarose gel and visualized with ethidium bromide under UV illumination. If the released fragment migrated near the 330 base pair marker it was considered to be the mu receptor cDNA clone. The cells which possessed the monkey mu receptor clone were grown in 500 ml of LB medium containing ampicillin overnight. The plasmids were isolated using the Qiagen plasmid isolation method. Briefly, the cells were separated from medium by centrifugation and lysed in 0.2 N NaOH and 1% SDS. Sodium acetate (4 M, pH 4.8) was added, mixed gently and centrifuged. The supernatant was placed on to the Qiagen columns and the plasmid collected, precipitated in isopropanol and centrifuged. The plasmids were washed in 70% ethanol and stored in water at -20°C. The purified plasmid was then sequenced at the P30 core facility at the Oregon Regional Primate Research Center. Sequence analysis indicated that the clone was 98% homologous to the human mu receptor nucleic acid sequence and 97% homologous to the human mu receptor amino acid sequence. The sequence was 60% and 63% homologous with the human delta and kappa receptor DNA sequences, respectively.

in situ Hybridization

Probe Preparation: The mu receptor antisense probe was synthesized from the pGEMT-MOR recombinant by linearizing with Pst I and transcribing with T7 RNA polymerase at 37°C for one hour (Maxiscript, Ambion, Inc.). Sense RNA was transcribed after Nco I linearization of pGEMT-MOR using SP6 RNA polymerase at 42°C for one hour. The [³⁵S]-UTP labeled sense and antisense probes were purified over NICK columns (Pharmacia, Inc.) to a concentration of 2-3 X 10⁻⁶ dpm/µl.

in situ Hybridization protocol: The methods used, with modifications, have been previously published (Ronnekleiv, et al., 1991; Ronnekleiv, et al., 1989). Briefly, tissues were brought to room temperature, pretreated with 0.1 M triethanolamine (TEA) for 3 minutes followed by a 10 minute treatment in 0.25% acetic anhydride in 0.1 M TEA to reduce background. The sections were covered with 50 µl of hybridization buffer (66% formamide, 10% dextran sulfate, 1X Denhardt's, 200 mM NaCl, 10 mM Tris (pH 8.0), 1.25 mM EDTA, 125 µg/ml tRNA, 100 mM dithiothreitol) and allowed to prehybridize for 60 minutes at 57°C. The sections were then washed in 2.0 X SSC (saline-sodium citrate) buffer. The labeled probe was heat denatured at 90°C for 10 minutes, chilled on ice, diluted in hybridization buffer and used at a final concentration of 6.67×10^3 dpm/µl. The sections were covered with glass coverslips, sealed with DPX (Gallard & Schleisenger) and hybridized at 57°C for at least 18 hours. The sections were washed in three changes of 2.0 X SSC buffer at room temperature for five minutes each and then treated with RNase (20 µg/ml) for 30 minutes at 37°C. Washing continued in 2.0 X, 1.0 X, 0.5 X, 0.25 X SSC for 10 minutes each at approximately 50°C to a final stringency of 0.1 X SSC containing dithiothreitol (1 mM) at 63°C. The sections were dehydrated in 50, 80, 90% ethanol with 300 mM ammonium acetate followed by 100% ethanol for 2 minutes each.

Autoradiography: The slides were apposed to β-MAX Hyperfilm (Amersham) along with ¹⁴C microstrip standards, placed in light-tight autoradiography cassettes, and stored at 4°C for 11-14 days. The film was developed in D19 developer for 4 minutes, rinsed in water, placed in Kodak fixer for 5 minutes and washed in water. If the film indicated that the *in situ* hybridization reaction was working, emulsion autoradiography of the slides was performed. The slides were dipped in Kodak NTB3 liquid emulsion diluted 1:1 in distilled water, air-dried in a humid atmosphere for 3 to 5 hours, sealed in light tight containers with Drierite and allowed to incubate at 4°C for 14-21 days. The slides were developed in Kodak D19 developer, fixed in Kodak fixer, and counterstained with Gills' 3X

hematoxylin (diluted 1:12 with water). The slides were dehydrated in ethanol, cleared in xylene, and coverslipped with Entellan.

Control Experiments: Control experiments utilized [³⁵S]-UTP labeled sense probe for mu receptor in situ hybridization on adjacent tissue sections; washing of hybridized sections in increasing temperatures up to 89°C; RNase pretreatment of sections prior to probe hybridization, and in situ hybridization with the mu receptor probes followed by mu receptor immunocytochemistry on the same tissue section revealing colocalization of mu receptor mRNA and mu receptor protein (Ronnekleiv, unpublished observations).

Analysis: The slides were analyzed and photographed using bright- and darkfield microscopy (Leitz). The film was digitized using a Polaroid SC 35 scanner. These images were edited for contrast using Adobe Photoshop 3.0 and Freehand 5.0 (Macromedia) on a Macintosh Quadra 950. The illustrations were drawn in Freehand 5.0 from computer scans (HP ScanJet IIcx/T scanner) of the actual brain sections. The digitized image of the sections were edited in Photoshop 3.0 to achieve the greatest clarity and then the paths drawn in Freehand 5.0. Each illustration was used to represent the mu receptor mRNA signal in a single section in the 40 day fetus or a series of sections in the 60 day and 70 day fetus. The figures were printed on a Phaser printer (Tektronix, Inc.). The arbitrary designations of dense, moderate, and low *in situ* hybridization signal were derived from grain counting in the 70 day fetus. The grains were counted in approximately a 150 μm^2 area using darkfield illumination on a Leitz microscope, the Macintosh Quadra 960 computer, and software from Dr. Donald Clifton (Chowen, et al., 1991). To determine the number of cells containing mu receptor mRNA, a 150 μm^2 area was counted under brightfield illumination using an eyepiece square grid reticle on a Leitz Laborlux microscope. The total number of cells and the number of cells that contained autoradiographic grains were counted using a 25 X objective. The number of cells with grains divided by the number of cells per square were expressed as a percentage.

Binding Autoradiography

Tissue Treatment: The day 70 and day 150 fetuses were treated as described earlier in this section. After termination of pregnancy by Cesarean section at day 70 and day 150 of gestation, the fetal brains were dissected and soaked in 0.1 M sodium phosphate buffer containing 20% sucrose (pH 7.2) for two hours at 4°C. The brain dissections were then infiltrated with O.C.T. embedding medium, placed in Tissue-Tek cryomolds, frozen in -55°C isopentane, and stored in liquid nitrogen until cryostat sectioning at 15 µm was performed. The sections were thaw mounted on to positively charged glass microscope slides and stored at -80°C.

Specific and Non-specific Binding: This technique has been previously established for the fetal monkey brain but not yet published (Fang et al, submitted). Briefly, the tissue sections were brought to room temperature, air dried and then fixed in 0.5% paraformaldehyde (0.1 M phosphate buffer) for 5 minutes at room temperature, rinsed briefly in TEN buffer (50 mM Tris, pH 7.35; 120 mM NaCl; 1 mM EDTA) and placed in the incubation chambers. The sections were preincubated in 200 µl of TEN buffer with 100 µM GTP and 0.01% BSA for 20 minutes at room temperature. After briefly rinsing in 50 mM Tris buffer (pH 7.45), the tissue sections were incubated in 300 µl of the selective mu opioid agonist [³H]-DAMGO (4 nM solution containing 0.01% BSA) for 90 minutes at 22°C. Nonspecific binding was evaluated by treating a parallel set of sections with the same concentration of [³H]-DAMGO in the presence of 5 µM naloxone (a non-selective opioid receptor antagonist). After incubation, the sections were gently washed in four changes of ice cold 50 mM Tris buffer (pH 7.45) containing 0.01% BSA for 20 seconds each followed by a final rinse in ice cold Milli-Q water for 10 seconds. The sections were rapidly dried under a stream of cool air and then kept at room temperature for at least three hours to insure complete drying.

Film Autoradiography: The slides were apposed to ³H-Hyperfilm (Amersham) along with [³H]-microscale standards (Amersham) and sealed in foil wrapped autoradiography

cassettes. They were stored for 4-6 weeks at 4°C in a light tight box. The film was then removed and developed in Kodak D-19 for 3 minutes followed by fixation in Kodak fixer for 5 minutes. The slides were then stained with Nissl stain for anatomical resolution.

Analysis: The films containing the images of the tissue sections along with the autoradiographic [³H]-microscale standards were scanned using the HP DeskScan/IIc SCT scanner. NIH Image 1.54 imaging program was used to determine the optical density of [³H]-DAMGO binding in each section. The optical density was converted to nCi/g using the standard [³H]-microscale standards (Amersham). The nonspecific binding density was subtracted from the total density and the values for specific binding were averaged. In each brain area, images were illustrated in Adobe Photoshop 3.0 from the scanned film images.

Results

Fetal Growth

Two fetuses were used for each fetal age group studied with the exception of the day 150 in which only one fetus was obtained. The body weights, crown-rump lengths, head circumference and in the 70 and 130 day fetuses, the brain weights were taken after the termination of pregnancy by Cesarean section and are presented in Table I. The amount of brain growth between day 70 and day 130 of fetal development is seen when comparing the two fold increase in head circumference compared with the nine fold increase in brain weight (Table I).

Morphological Maturation of the Fetal Monkey Brain

Day 40 and Day 45 fetal rhesus monkey

At day 40 of gestation, the telencephalic hemispheres were comprised of the frontal and temporal lobes with the latter enveloping the dorsomedial aspect of the diencephalon (Fig. 1 A-D). The ganglionic eminence was apparent in the floor of the lateral ventricles. The choroid plexus had begun to develop in the medial wall of the lateral ventricle and was projecting into the ventricle itself. In the diencephalon, the epithalamus, thalamus, and hypothalamus surrounded the third ventricle which was continuous throughout the diencephalon. Dorsally, the epithalamus consisted of a relatively thin layer of cells which extended ventrally to join the dorsal thalamus (Fig. 1 B-D). The dorsal thalamus was comprised of a thin layer of densely packed cells approximately twelve cells thick which lined the ventricle, the proliferative ventricular zone, and was continuous with a layer of cells that were less densely packed. Lateral to this was another layer of densely packed cells approximately ten to twenty cells thick. The dorsal thalamus was separated from the ventral thalamus by an area which contained fewer cells. In the ventral thalamus, there was

a tightly packed layer of cells lining the ventricle that was so dense individual cells were difficult to distinguish. Lateral to this, the individual cells were recognizable, but densely packed. The ventral thalamus was distinguishable from the hypothalamus by a layer of cells that were less concentrated. Medially, the hypothalamus contained a layer of cells next to the ventricle that was continuous with the thickly packed cells in the body of the hypothalamus in which individual nuclei could not be distinguished.

In the 45 day fetus, there were a few changes morphologically compared to the 40 day fetus. The ganglionic eminence, which was seen as a single protrudence in to the lateral ventricle of the 40 day fetus, could be divided into lateral and medial ridges in the 45 day fetus. The choroid plexus had grown and filled up more of the lateral ventricles. The entire area of the brain had increased in the 45 day fetus, but the characteristics described for the 40 day fetus held true for this stage of development.

Day 60 fetal rhesus monkey

In comparison to days 40 and 45, the brain of the 60 day fetal monkey had developed substantially (Fig. 2). The telencephalic hemispheres had grown out laterally and caudally to include the frontal, temporal, parietal, and occipital lobes. The caudate was located directly under the ganglionic eminence in the rostral brain. The caudate and putamen were separated by the internal capsule yet the two nuclei were connected by strands of cells bridging this structure. Both nuclei consisted of densely packed cells. The putamen was distinguishable from the surrounding cortex which had a less dense cellular concentration. The septum consisted of a dense layer of cells at the lateral ventricular surface which became more sparse medially. In the more ventral septal areas, the cell density increased and was fairly evenly distributed up to the pial boundary. The olfactory bulbs were continuous with the telencephalic floor and did not yet have distinct layers although the cells appeared to have a circular orientation. In the diencephalon, the habenula was characterized by the compact layer of cells in the medial portion and the less compact region of the lateral habenula. In the thalamus, the third ventricle was lined with a thin layer of

densely packed cells which were continuous with a somewhat densely packed cellular layer that was approximately 250 μm in width. The mediodorsal thalamic area appeared as a fairly homogenous layer of cells that was bordered by the reticular nucleus ventrally and laterally. The reticular nucleus was distinguishable from the rest of the thalamus due to the less densely packed cells. Caudally, the ventrolateral nucleus was distinct from the more medial nuclei due to its dense cell structure. The hypothalamus had distinct nuclei that were distinguishable due to the heterogeneous cellular density. In the mesencephalon, the aqueduct was much smaller compared to the day 40 fetus, and was surrounded by the periaqueductal gray. The superior colliculus was just dorsal to the periaqueductal gray. The intermediate and superficial layers were quite dense and very distinct. The reticular formation was characterized by the relative sparsity of cells that were almost spotty in appearance. The raphe, however appeared as distinct nuclei. The nucleus of the lateral lemniscus was also distinctive due to the cell density. In the caudal brain, the cochlear nucleus could be discerned just medial and ventral to the proliferative rhombic lip (Fig. 2H). The nucleus of the spinal trigeminal nucleus and the inferior olivary nucleus were also distinctive due to their cell densities compared to the surrounding areas which had fewer cells (Fig. 2 G-I). The midline from the fourth ventricle to the ventral surface of the medulla was a cell poor zone.

Day 70 fetal rhesus monkey

In the rostral brain at day 70 of gestation, the lateral ventricle had become a thin slit and was lined by a thick layer of cells which surrounded the caudate nucleus on the dorsal and medial sides (Fig. 3). The caudate was clearly distinguishable from the ganglionic eminence due to the less dense cellular distribution. Just under the ganglionic eminence there were small groups of cells which clustered together and extended into the caudate. The putamen appeared fairly homogenous. The septum was characterized by a sparse layer of cells on the pial border that was continuous with the cell dense region of the medial septum. This was flanked laterally by the lateral septum which contained fewer cells and at

the most lateral boundary, had a layer of cells which seemed to be oriented in a vertical direction. At the ventral border of the lateral ventricle in the area of the nucleus accumbens, there were layers of cells three to four cells thick which spread ventrally and medially (Fig. 3 B). In the diencephalon, the ganglionic eminence was located in the floor of the thinning lateral ventricle just dorsal to the caudate nucleus and was distinguished by the density of the cells. The internal capsule had increased in size and the proliferative zone of the third ventricle was now absent. The anterior nuclei and the ventrolateral nucleus of the thalamus were distinguishable and the mediodorsal nucleus was ovoid in structure in the middle of the thalamus. The thalamus was encased by the reticular nucleus ventrolaterally. The hypothalamus was fairly homogenous medially with regards to cell density yet laterally the cell density decreased. The third ventricle is no longer open due to the expansion of the midline thalamic nuclei. The amygdala appeared as a cell dense region in the temporal lobe at the level of the hypothalamus (Fig. 3 C, D, E). A large dense cluster of proliferative cells was found just dorsal to the hippocampus. As the hippocampus began to curl dorsally and medially, this dense cellular zone persisted into the outer layers of the hippocampus proper. In the mesencephalon, the interpeduncular and the raphe nuclei and the ventral tegmental areas were all seen as distinct cell groups (Fig. 3 H). The pulvinar, which is actually a caudal thalamic nucleus, could also be distinguished as a separate nucleus. The pons could be distinguished from the midbrain based on its location and increased cell density. The pineal gland was very distinct and cell dense. The periaqueductal gray had more cells in its dorsal regions than it did ventrally. The cerebellum had expanded compared to the 60 day fetus and was clearly seen between and lateral to the inferior colliculi (Fig. 3 J, K, L). The cerebellum was relatively smooth in appearance although cell dense layers had begun to appear under the external layers. The superior and inferior olivary nuclei were distinct with the latter first appearing as a dense group of cells on either side of the midline ventrally (Fig. 3 K, L). The cochlear was also distinct and fairly cell dense (Fig. 3 L). The choroid plexus of the fourth ventricle was quite extensive. The cell

dense rhombic lip was still apparent at the lateral confines of the fourth ventricle. The spinal nucleus of the trigeminal also appeared as a cell rich structure along with the nucleus ambiguus (Fig. 3 J, M).

Day 130 and day 150 fetal rhesus monkeys

By 130 days of gestation, the brain had increased in size to such an extent that it had to be dissected in blocks. For this study only the thalamus was used in this age group. It was possible to distinguish between the nuclei of the thalamus based on the cell density and location. The reticular nucleus encased the entire thalamus and could be readily identified based on the low cell density in this nucleus compared to the more medially situated nuclei. The day 150 fetal brain had increased in size compared to the 130 day fetal brain with the most noticeable features being the discrete maturation of individual nuclei, based on cellular density and location, and the increased area of the cortex.

Mu Receptor mRNA in the Fetal Monkey Brain

Day 40 and 45 fetal rhesus monkeys

Autoradiographic grains, indicative of mu receptor mRNA were observed in the developing diencephalon, the pons, cerebellar plates and the brainstem (Figs. 1, 4). At this stage of development, mu receptor mRNA was not found in the telencephalon. In the diencephalon, which had the highest concentration of autoradiographic grains, mu receptor mRNA containing cells were located in the ventral thalamus just lateral to the ventricular zone. The proliferative layer of cells did not contain any mu receptor mRNA (Fig. 1 B-D; Fig. 4 B, C). When counting the cells that contained autoradiographic grains within a 150 μm^2 area in the ventral thalamus, approximately 50% of the cells were labeled with five to twenty grains per cell compared to zero to two grains per cell in other areas (Table IV). Due to the dense packing of the cells, the signal in the ventral thalamus appeared quite intense in darkfield photomicrographs (Fig. 4 B, C). There was no apparent rostral to caudal gradient of mu receptor mRNA as it was located in the ventral thalamus throughout

the extent of the diencephalon. In the differentiating fields of the pons, mu receptor mRNA containing cells were found laterally in the nucleus of the spinal trigeminal (Fig. 1 D). The mesencephalon did not contain appreciable amounts of mu receptor mRNA. The cerebellar plates had autoradiographic grains located in the layer adjacent to the proliferative zone of the fourth ventricle (Fig. 1 E). A faint signal for mu receptor mRNA was also seen dorsal to this in the arms of the cerebellar plates which connect it to the mesencephalon at this stage in development (Fig. 4 D). In the brainstem, a faint but specific signal for mu receptor mRNA was present in the various nuclei along the midline. The same pattern of labeling for mu receptor mRNA was seen in the 40 and 45 day fetuses although, as mentioned earlier, the brain size of the 45 day fetus was larger.

Day 60 fetal rhesus monkey

The day 60 fetal brain had increased greatly in size and not only were individual nuclei recognizable, due to increased cell density, but in the rostral regions of the diencephalon, the third ventricle had closed in its dorsomedial aspects. This was indicative of the maturation of the brain over the fifteen to twenty days from the day 40 and 45 fetuses in which the brain was essentially tubular (Figs. 1, 2). In the telencephalon, mu receptor mRNA was observed in the evaginating olfactory bulbs and in the medial and lateral septum including the putative diagonal band and the nucleus accumbens (Fig. 6 A, B). In the striatum, mu receptor mRNA was detectable, although faintly, in the patches of the putamen with no specific signal found in the matrix (Figs. 2; 6 B). Mu receptor mRNA was found on the lateral and ventral edges of the putamen, which corresponds to the subcallosal streak in the rat (Figs. 2; 6 B). In the diencephalon, the highest density of grains was found in the medial habenula and the reticular nucleus of the thalamus (Figs. 2; 6 C; 8 A; 10 A). In a 150 μm^2 area encompassing the medial habenula, approximately 30% of the cells were labeled for mu receptor mRNA (Table IV). In the reticular nucleus of the thalamus, 37% of the cells contained autoradiographic grains for mu receptor mRNA (Table IV). The number of grains per cell were difficult to determine but ranged from ten

to twenty in both nuclei. It should be noted that in Figure 8 A, the brightfield photomicrograph was taken at the lateral edge of the medial habenula where the cells did not appear as dense as they did in the more medial aspects of this nucleus. The mu receptor mRNA in the reticular nucleus of the thalamus was seen in the ventrolateral aspects of the nucleus rostrally and in the more caudal areas, the signal was also seen ventromedially. Mu receptor mRNA was found in the putative anteromedial nucleus and caudal to this in the mediodorsal nucleus of the thalamus (Fig. 2). In the latter, approximately 23% of the cells in a 150 μm^2 area were labeled for mu receptor mRNA (Table IV). The intermediate gray of the superior colliculus was also found to have mu receptor mRNA. In the rostral part of the mesencephalic reticular formation, mu receptor mRNA was seen in a diffuse, but specific, area medially and laterally (Fig. 2 F). Moving caudally, the signal in the reticular formation was more medial (Fig. 2 G). There was also a faint signal for mu receptor mRNA detected in the raphe nucleus. The nucleus of the lateral lemniscus contained a strong signal for mu receptor mRNA (Fig. 2 G; 9 A, B). The cells in this nucleus were more dense than the cells in the area surrounding the nucleus but they were not packed together and individual cells were clearly distinguishable (Fig. 9A). The autoradiographic grains appeared diffuse but were well within the boundaries of the lateral lemniscus nucleus (Fig. 9 B). In the metencephalon and the myelencephalon, the cochlear nucleus contained mu receptor mRNA as did the inferior olivary nucleus (Fig. 2 H). The spinal trigeminal nucleus was also found to express mu receptor mRNA although the signal was slightly lower than that seen in the cochlear or the inferior olivary nucleus (Fig. 2 H, I), The nucleus of the solitary tract contained mu receptor synthesizing cells with autoradiographic grains comparable to those seen in the spinal trigeminal nucleus (Fig. 2 I). There was no mu receptor mRNA detected in the cerebellum at this stage of development.

Day 70 fetal rhesus monkey

Brain development in the 70 day fetus had progressed substantially compared to the 60 day fetus and many additional nuclei contained mu receptor mRNA. In the

telencephalon, mu receptor mRNA was expressed in the granular layer of the olfactory bulbs (Figs. 3 A; 7 B). Like the 60 day fetus, the medial and lateral septum both expressed mu receptor mRNA as well as the areas of the diagonal band and the nucleus accumbens (Fig. 3 B). In the putamen, the patchy distribution of mu receptor mRNA was more prominent compared to the 60 day fetus (Fig. 7 A). These patches are not distinguishable anatomically when examining Nissl stained sections and are only characterized biochemically. In the diencephalon, mu receptor mRNA was found in the now discernible paraventricular nucleus of the thalamus (Fig. 3 C; 11 A, B). The autoradiographic grains were located adjacent to the ventricular cleavage of the dorsal thalamus in cells that were moderately dense but distinctive in appearance (Fig. 11 A). A moderate amount of mu receptor mRNA was observed in the mediodorsal and laterodorsal nuclei of the thalamus and a dense signal seen in the ventrolateral nucleus (Fig. 3 C-F). The thalamic reticular nucleus contained dense autoradiographic grains for mu receptor mRNA (Fig. 7 C; 10 C, D). Compared to the 60 day fetus, the cellular density of the reticular nucleus was less and the individual cells were larger in the 70 day fetus. The mu receptor mRNA grains were also more dense over individual cells in the 70 day versus the 60 day fetus (Fig 10 C, D). In a $150 \mu\text{m}^2$ area, the number of cells which contained mu receptor mRNA was approximately 75% whereas in the 60 day fetus it was 37% (Table IV). Mu receptor mRNA was also observed in the centromedian and centrolateral nuclei of the thalamus (Fig. 3 G; 12 A, B). In the centromedian nucleus, 60% of the cells in a $150 \mu\text{m}^2$ area contained mu receptor mRNA. In the centrolateral nucleus, the autoradiographic grains appeared dense but diffuse across the nucleus and the cells were fairly close together with the grain density within each cells was substantial (Fig. 12 A, B). In the hypothalamus, mu receptor mRNA was observed in the paraventricular nucleus, the dorsomedial nucleus, the lateral hypothalamic area and in the arcuate. The signal was faint for all of these areas (Fig. 3 C, D). Dense mu receptor mRNA signal was observed in the medial habenula (Fig. 3 F-H; 8 C, D). In comparison to the 60 day fetus which had 29% of the cells in the medial

habenula containing mu receptor mRNA, the 70 day fetus had 67.1% of the cells in a 150 μm^2 area which contained mu receptor mRNA (Table IV). Unlike the 60 day fetus, in the 70 day fetal monkey, mu receptor mRNA was detected in the amygdala although the individual nuclei of this structure could not be distinguished (Fig. 3 C-E). The hippocampus, too, contained cells expressing mu receptor mRNA for the first time at day 70 of development. The cells which concentrated grains were in the CA3 region of the hippocampus (Fig. 3 F-H). In the mesencephalon, the substantia nigra expressed mu receptor mRNA as did the interpeduncular nucleus, the raphe nucleus and the ventral tegmental area although the signal in the latter three was faint but specific (Fig. 7 D, E). Mu receptor mRNA was also seen in the nucleus of the lateral lemniscus and the central nucleus of the inferior colliculus as well as the nucleus of the spinal trigeminal (Fig. 3 H, I; 7 F). In the metencephalon, there was a fairly dense signal for mu receptor mRNA seen in an area immediately lateral to the locus coeruleus and was thought to be the nucleus of the spinal trigeminal (Fig. 7 H). In the myelencephalon, relative moderate amounts of mu receptor mRNA were observed in the cochlear nucleus, the nucleus of the solitary tract and the inferior olivary nucleus and there was also a faint diffuse signal seen in the reticular formation (Fig. 3 K, L). Mu receptor mRNA was also quite distinctive in the developing ventral raphe nuclei (Fig. 7 G; 3 K, M). There was a dense signal for mu receptor mRNA found in the nucleus ambiguus. The cerebellum displayed faint expression of mu receptor mRNA in the areas of the deep nuclei.

Day 130 fetal rhesus monkey thalamus

In the 130 day fetus, only the thalamus was available for in situ hybridization analysis. The thalamus had matured considerably compared to the day 70 fetus as evidenced by the striking increase in size. Mu receptor mRNA was found in the paraventricular nucleus, the reticular nucleus, the centrolateral and the laterodorsal nuclei. In the paraventricular nucleus, mu receptor mRNA was distinctly localized to individual cells (Fig. 11 C, D). In comparison to the 70 day fetus, the number of cells per area had

decreased whereas the signal per cell for mu receptor mRNA had increased (Fig. 11 C, D). In a 150 μm^2 area, 41% of the cells contained mu receptor mRNA (Table IV). In the centrolateral nucleus, this same pattern of fewer cells per area yet more grains per cell was seen when comparing the 130 day fetus with that of the day 70 fetus (Fig. 12 C, D vs. A, B). This general trend of fewer cells per area yet more autoradiographic grains for mu receptor mRNA is perhaps best illustrated in the reticular nucleus which expressed mu receptor mRNA in the days 60, 70, and 130 fetuses (Fig. 10 A-F). It was readily apparent that the reticular nucleus contained fewer cells per area by day 130 of development and the signal for mu receptor mRNA had become restricted to individual cells (Fig. 10 E, F).

[³H]-DAMGO Binding of Mu Receptor in the 70 and 150 Day Fetal Monkey

Contrasting mu receptor binding in days 70 (n=3) and 150 (n=1) fetal monkey brain is essentially a comparison between the first and second halves of gestation. After measuring the optical densities from autoradiographic film of tritiated DAMGO binding to fetal brain sections, the following density categories were determined: low binding = 0-1000 nCi/g; moderate binding = 1000-2000 nCi/g; Dense binding = 2000-3000 nCi/g; and very dense binding \geq 3000 nCi/g.

In the telencephalon of the day 70 fetal monkey, binding varied from very low to moderate as illustrated in Table II and Table III. The lowest mu receptor binding densities were observed in the frontal and cingulate cortex, the olfactory bulbs, the septum, and the putamen. All of these areas had optical densities below 300 nCi/g. The caudate and the globus pallidus had low optical densities and the amygdala had moderate optical densities (Fig. 13 A, B, C). Mu receptor binding in the caudate and the putamen were patchy in appearance with the patches containing a slightly higher binding density in comparison to the surrounding matrix although matrix binding was also apparent (Fig. 13 A). The diencephalon contained the highest density of mu receptor binding in the day 70 fetal brain. At this stage of development, the mediodorsal, centrolateral and the reticular nuclei of the

thalamus had the most dense binding (Fig. 13 B, C). The ventrolateral and paraventricular nuclei of the thalamus had dense mu receptor binding. The medial geniculate displayed moderate mu receptor binding densities (Fig. 13 D, Table II). The hypothalamus was characterized by low binding densities which appeared fairly homogenous throughout most of its extent with the exception of the arcuate and the supraoptic nuclei. These latter two nuclei were found to have moderate binding densities for mu receptor (Table II). In the mesencephalon, the most intense binding was found in the fasciculus retroflexus, the superior colliculus, and the periaqueductal gray (Fig. 13 D, Table II). The substantia nigra and the reticular formation both had moderate mu receptor binding densities (Fig. 13 D, Table II). In the metencephalon, moderate binding densities were observed in the pontine reticular and pontine raphe nuclei, parabrachial nucleus, dorsal tegmental area, the sensory and motor nuclei of the spinal trigeminal, and the cochlear nucleus (Fig. 13 E, Table II). Low mu receptor binding was found in the deep cerebellar nuclear areas and in the cerebellar cortex (Fig. 13 E, Table II). Dense binding was observed in the inferior olivary nucleus (Fig. 13 E, Table II).

In the 150 day fetal monkey, mu receptor binding in the septum was low (Fig. 14 A, Table II). In the caudate and the putamen, mu receptor binding was patchy in appearance with the patches found to have moderate binding densities compared to the low binding seen in the matrix (Fig. 14 A; Table II). The external segment of the globus pallidus also had moderate binding densities (Table II). This was contrasted to the very low levels of binding in the internal segment of this same nucleus (Fig. B, Table II). There was no binding in the optic tract (Fig. 14 B, Table II). In the diencephalon, the most dense areas of binding were found in the paraventricular and laterodorsal nuclei of the thalamus. The ventrolateral, mediodorsal, and reticular nuclei of the thalamus also had very dense mu receptor binding but still less than that of the paraventricular and laterodorsal nuclei (Fig. 14 B, Table II). The ventromedial and ventrolateral nuclei were found to contain very dense mu receptor binding (Fig. 14 C, Table II). The dorsomedial, ventromedial and

arcuate nuclei of the hypothalamus were observed to express very dense mu receptor binding densities (Table II). In the mesencephalon, the fasciculus retroflexus had very dense mu receptor binding and the substantia nigra had low binding levels (Fig. 14 C, Table II). There was no signal detected in the cerebellar peduncles. The superior colliculus and the periaqueductal gray had moderate mu receptor binding densities as did the linear raphe nucleus (Fig. 14 D, Table II). The pontine reticular nucleus had very dense mu receptor binding sites (Fig. 14 D, Table II). In the metencephalon, the cochlear had dense mu receptor binding sites yet the caudal inferior colliculus and the reticular formation displayed a low density, homogeneously distributed signal for mu receptor binding (Fig. 14 E). The cerebellum did not contain binding sites for mu receptor in the cortex. The deep nuclear areas of the cerebellum were not examined in the 150 day fetus. In the caudal brain, mu receptor binding sites were observed in the nucleus of the spinal trigeminal whereas the inferior olivary nucleus had moderate binding densities (Fig. 14 F, Table II).

In comparing the mu receptor binding in the 70 and 150 day fetuses, with the exceptions of the striatum, the reticular nucleus of the thalamus, the periaqueductal gray, the inferior olivary nucleus and the spinal trigeminal nucleus, the binding densities for mu receptor were more dense in the 150 day fetus (Fig. 15, Table II). In the striatum of both the day 70 and day 150 fetus a patchy distribution of mu receptor binding was found but the overall binding density of this structure was approximately equal between the two age groups. This was also true for binding densities in the thalamic reticular nucleus, the periaqueductal gray and the nucleus of the spinal trigeminal. In the inferior olivary nucleus, the mu receptor binding was less dense in the 150 day fetus compared to the day 70 fetus (Fig. 15, Table II).

Mu Receptor mRNA and Mu Receptor Binding in the 70 Day Fetal Monkey

In the day 70 fetus, telencephalic mu receptor mRNA and mu receptor binding sites were both expressed in the olfactory bulbs, the patches of the putamen, the subcallosal streak,

the septum, and the amygdala (Table III). The amygdala exhibited dense mu receptor mRNA and although the mu binding densities were moderate they were the highest seen in the telencephalon. The olfactory bulbs also exhibited a strong signal for mu receptor mRNA in the granular layer yet only low binding densities were seen in this layer (Fig. 3 A; 7 B; 13 A, Table III). There was, however, no mu receptor mRNA expressed in the frontal cortex or in the globus pallidus which contrasted to the expression of mu receptor protein seen in these areas (Fig. 3 A, B; 7 A, B; 13 A; Table III). In the thalamus, mu receptor binding sites were the most dense in the reticular and the mediodorsal nuclei with very dense binding also seen in the laterodorsal, centrolateral, centromedian, and paraventricular nuclei (Fig. 13 C, Table III). Mu receptor mRNA was observed in all of these nuclei with the most intense signal in the reticular, centrolateral and anteromedial nuclei of the thalamus (Fig. 3 C-E; 10 C, D; 11 A; 12 A, B; Table III). Although there was mu receptor binding in the medial geniculate, no mu receptor mRNA was found in this nucleus. In the hypothalamus of the 70 day fetus, mu receptor binding sites were found in all areas which express mu receptor mRNA including the supraoptic, paraventricular, dorsomedial nuclei, the lateral hypothalamic area and the arcuate nucleus (Fig. 3 C, D; Table III). There was also moderate binding in the mammillary nucleus but no corresponding mu receptor mRNA expressed. Unlike mu receptor mRNA which was located in discrete regions, mu receptor binding was seen throughout most of the hypothalamic area (Fig. 13 B). In the epithalamus, mu receptor binding sites and mRNA were dense in the medial habenula with virtually no binding or mRNA in the lateral habenula (Table III). In the mesencephalon, mu receptor mRNA and mu receptor binding were seen in the substantia nigra, ventral tegmental area, interpeduncular nucleus, and the superior and inferior colliculi. Although there was moderate mu receptor binding density in the periaqueductal gray, mu receptor mRNA expression was almost undetectable. There were also dense mu receptor binding sites but no mu receptor mRNA in the fasciculus retroflexus (Fig. 13 G; 3 H, I; 7 D-F; Table III). There was low homogenous binding in

the region of the nucleus of the lateral lemniscus but a strong signal for mu receptor mRNA (Fig. 9 C, D; Table III). In the metencephalon and myelencephalon, the correspondence between mu receptor binding and mu receptor mRNA varies. Mu receptor mRNA was found in the nucleus of the lateral lemniscus and the nucleus of the spinal trigeminal. Mu receptor binding was seen in the latter but not in the former. There was mu receptor binding in the cerebellar cortex, an area which does not contain mu receptor mRNA although, a slight signal for mu receptor mRNA and binding was found in the deep nuclei (Fig. 3 J-L; 13 E; Table III). There were also mu receptor binding sites in the parabrachial and the locus coeruleus, areas which only contain a faint signal for mu receptor mRNA. The mesencephalic nucleus of the spinal trigeminal is just lateral to the locus coeruleus and contained a strong signal for mu receptor mRNA (Fig. 7 H). Mu receptor mRNA and binding are both located in the cochlear and the inferior olivary nucleus (Fig. 3 L; 13 E).

Discussion

The development of the mu opioid receptor was studied in the fetal rhesus monkey at gestational days 40, 45, 60, 70, 130, and 150 of a 165 day gestational period using in situ hybridization (E40, E45, E60, E70, E130) and [3H]-DAMGO binding autoradiography (E70, E150). The primary findings of this investigation are as follows.

1) Mu receptor mRNA containing cells were found in the fetal monkey brain by day 40 of gestation. 2) In the day 60 and the day 70 fetal brain, mu receptor mRNA was more widely expressed with a very distinct signal seen in the reticular nucleus of the thalamus. 3) By day 70, fetal striatal mu receptor mRNA was expressed within the striosomal boundaries. 4) In the day 70 fetal brain, mu receptor binding sites corresponded well with the distribution of mu receptor mRNA. 5) Mu receptor binding densities in the first and second halves of gestation were, for the most part, similar.

Mu Receptor mRNA during Fetal Development

This is the first study of mu receptor mRNA localization in the fetal primate brain. In the day 40 fetal monkey, the most rostral brain region expressing mu receptor mRNA is the ventral thalamus of the developing diencephalon. This area also displays the most intense mu receptor mRNA signal seen at this stage of development in the monkey. The mu receptor mRNA containing cells were located adjacent to the proliferative zone but not within it. Mu receptor mRNA was expressed in the diencephalon of the mouse at E13.5 of a twenty day gestational period, an embryonic stage which is comparable to the day 40 fetal monkey (Gribnau & Geijsberts, 1981). Mu receptor mRNA was also found in the hypothalamus and the caudate-putamen in the fetal mouse at this time, which is not seen in the 40 day fetal monkey (Zhu, et al., 1995; Zhu, et al., 1996). In the fetal rat, the earliest thalamic structure to develop is the reticular nucleus which appears on E13 of a 21 day gestation period (Altman & Bayer, 1988a; Altman & Bayer, 1988b). It is tempting to speculate that the signal seen in the fetal monkey thalamus could incorporate the reticular

nucleus but this cannot be stated definitively as no description of the early ontogeny of the primate reticular nucleus is available. In the developing rat brain, the dorsal and ventral thalamus occupy the dorsal half of the diencephalon compared to the 40 day fetal monkey brain where the dorsal and ventral thalamus occupy approximately two thirds of the diencephalon with the hypothalamus residing in the ventral third (Altman & Bayer, 1988a; Gribnau & Geijsberts, 1981; Gribnau & Geijsberts, 1985). However, based on information of the development in the fetal rat thalamus, the ventral thalamus in the monkey probably gives rise to the reticular nucleus and the mediodorsal nucleus of the thalamus in the monkey. There were no mu receptor mRNA containing cells found in the telencephalon at day 40 of gestation in the monkey. This is in contrast to the rat where mu receptor mRNA and naloxone binding were detected in the striatal anlage on E14, which is comparable to days 34-42 in the fetal monkey (Chabot, et al., 1995; Gribnau & Geijsberts, 1981; Kent, et al., 1982). Mu receptor mRNA was also found in the basal telencephalon of the mouse at E12.5 (Zhu, et al., 1996). Mu receptor mRNA in the fetal monkey was also located in the cerebellar plates, the differentiating field of the pons and in the brainstem which is in agreement with that found in the mouse at E13.5, a comparable stage of development (Zhu, et al., 1995). The migrating neurons of the fetal monkey possess mu receptor mRNA during the first quarter of gestation whereas, the rodent does so in the second half of gestation although at developmental stages earlier than those seen in the fetal monkey in this study. β -endorphin immunoreactivity, β -endorphin being an endogenous ligand for the mu receptor, has been shown in the arcuate nucleus of the fetal monkey by day 38 of gestation (Ronnekleiv, unpublished observations) and as early as E13 in the fetal rat (McDowell & Kitchen, 1987).

Gestational day 60 of the fetal monkey is the earliest time point in which mu receptor mRNA was seen in the telencephalon, specifically the olfactory bulbs, septum, and the striatum. This is of particular interest with regard to the striatum. Mu receptor mRNA is located within the striatal striosomes or patches at day 60 although the boundaries

of this compartment are not clearly delineated until day 70 of gestation in which the elongate and convoluted striosomal pattern of the adult is seen (Gerfen & Wilson, 1996). This is not the case in the rat in which mu receptor is expressed as early as E14, yet the compartmentalization of the receptor into the striosomes is not apparent until the day of birth and does not attain the adult pattern of distribution until the second postnatal week (Edley & Herkenham, 1984; Kent, et al., 1982). The cells of the primate striatum appear between E36 and E80 in well defined clusters which indicates that the striosomes are the first cells born to the striatum, a condition which is also seen in the fetal rat (Brand & Rakic, 1979; van der Kooy & Fishel, 1987). The developmental pattern of striatal maturation therefore differs between the primate and the rodent. In the monkey, there was a gradual increase in striatal mu receptor synthesizing cells which attained the adult distribution during the first half of gestation. In the rodent, adult concentrations of mu receptor are seen early in development yet the adult distribution is not attained until after birth. In humans, the striatum plays an important role in the execution of learned procedural skills requiring motor output, such as riding a bicycle, and has a participatory role in language and speech articulation (Ilinsky & Kultas-Ilinsky, 1995; Tranel, 1995). Phylogenetic order could be one of the reasons that the developmental patterns seen in the striatum differs between the rodent and the primate.

In the day 60, day 70, and day 130 fetal monkeys, the reticular nucleus of the thalamus exhibits an intense signal for mu receptor mRNA. There has been no literature available on mu receptor localization in the reticular nucleus of the fetal rat. However, in the adult rat, there was no binding or mRNA found in this thalamic nucleus (Delfs, et al., 1994a; Mansour, et al., 1988). In rats, cats, and monkeys, the reticular nucleus surrounds the thalamus and is unique in that although it has no direct connection with the cortex, it receives collaterals from all corticothalamic and thalamocortical projections and in turn has reciprocal projections to ipsilateral (and a few contralateral) dorsal thalamic nuclei (Battaglia, et al., 1994; Jones, 1975; Kolmac & Mitrofanis, 1997; Lozsadi, 1994; Ohara &

Lieberman, 1985). The dorsal thalamic nuclei to which the reticular nucleus projects include the mediodorsal, anteromedial, centromedian, centrolateral, laterodorsal and paraventricular nuclei which participate in limbic, motor, or arousal behavioral systems (Ilinsky & Kultas-Ilinsky, 1995; Kolmac & Mitrofanis, 1997; Lozsadi, 1994). All of these nuclei contain mu receptor mRNA and binding sites in the fetal monkey. The reticular nucleus also receives projections from the mesencephalic reticular formation, pedunculopontine tegmental nuclei, parabrachial, substantia nigra, and the ventral tegmental area and therefore participates in the coordination of attention and arousal states (Cornwall, et al., 1990; Pare & Steriade, 1993). All of these areas contain mu receptor in the fetal monkey. The specific role of the mu receptor in each of these regions is not well known. The medial column of the reticular formation sends ascending projections to the centromedian nucleus of the thalamus which both participate in the reticular activating system (McCarley, 1995). Collaterals are also sent to the reticular nucleus of the thalamus from the limbic system including the hippocampus, septum, and amygdala which would indicate a participatory role in emotional behaviors and memory (Ilinsky & Kultas-Ilinsky, 1995). The corticoreticular neurons utilize the neurotransmitters glutamate and aspartate which are excitatory. The neurons of the reticular nucleus, many of which are GABAergic, then send inhibitory impulses to dorsal thalamic nuclei (Lozsadi, 1994; Lozsadi, 1995). It is highly probable that the mu receptor provides inhibitory input to the GABAergic neurons of the reticular nucleus to function in a coordinating or regulatory capacity between cortical, subcortical, and thalamic input and output circuits.

In the 60 and 70 day fetal monkey, mu receptor mRNA was found in a variety of midbrain and brainstem nuclei which participate in motor and sensory functions. In the auditory pathway of humans and guinea pigs, for example, the dorsal cochlear nucleus sends projections through the nucleus of the lateral lemniscus to the inferior colliculus and then to the acoustic area of the temporal lobe via the medial geniculate nucleus of the thalamus (Netter, 1986; Schofield & Cant, 1997). Mu receptor containing cells are found

in the cochlear, nucleus of the lateral lemniscus and the inferior colliculus. The superior colliculus, which participates in visuomotor functions, receives afferent projections from the spinal trigeminal, inferior colliculus, substantia nigra, and the deep cerebellar nuclei, all of which contain mu receptor mRNA expressing cells (Spencer, 1995). The inferior olivary nucleus has reciprocal connections with the cerebellum and participates in refined motor skills. Both nuclei contain mu receptor mRNA. The mu receptor could, therefore, participate in the modulation of sensory input and/or response to sensory stimuli and the associated motor responses.

Mu Receptor Binding during Fetal Development

In general, there is a good deal of correspondence between mu receptor binding sites and mu receptor mRNA in the fetal monkey brain. All areas which contain mu receptor mRNA contain mu receptor binding sites yet the reverse was not always true. This was illustrated by the lack of mu receptor mRNA in the frontal, cingulate, and piriform cortices which contain mu receptor binding sites in the fetal monkey. Another fetal monkey brain region which contained mu receptor binding but no mu receptor mRNA was the globus pallidus, which is one of the major targets of striatal afferent projections (Gerfen, 1992). This indicates that the mu receptor may be synthesized in the striatum and then transported to the globus pallidus. It could also be that mu receptor mRNA is below detectability. Mu receptor mRNA is present in relatively high quantities in the globus pallidus of the adult monkey. The caudate and putamen contain mu receptor binding sites distributed in the characteristic patchy pattern. The striatum also projects to the substantia nigra, the pedunculopontine nucleus, superior colliculus, and the intralaminar thalamus and utilizes GABA and dynorphin as the neurotransmitters (Gerfen, 1992; Gerfen & Wilson, 1996). The centromedian nucleus of the thalamus and the substantia nigra send reciprocal projections to the striatum (Gerfen, 1992; Gerfen & Wilson, 1996). It is therefore likely that the mu receptor participates in the modulation of this neural circuitry which is related to

motor activity. Also in the telencephalon of the fetal monkey, mu receptor binding sites were found in the olfactory bulbs and in all of the amygdala nuclei, areas which also contained mu receptor mRNA. This corresponds with findings in the adult rat with the exception of the central nucleus of the amygdala in which no mu binding sites were seen (Mansour, et al., 1995a). The functional significance of the expression of mu receptor in these structures is not known. It does, however, indicate that mu receptor could participate in the olfactory sensory pathway as well as the regulation of emotional control and expression since amygdaloid ablation in monkeys stimulates a variety of dysfunctions including emotive ones (Ilinsky & Kultas-Ilinsky, 1995). In rats, the central amygdala projects to the periaqueductal gray and when stimulated, results in analgesia and freezing behavior which is opioid dependent and due to the release of enkephalin (Da Costa Gomez & Behbehani, 1995). Mu receptor binding sites were also located in the periaqueductal gray of both the 70 and 150 day fetal monkeys which participates in nociceptive pathways. The thalamus of the fetal monkey contained the most mu receptor binding sites. This was also seen in the adult rat with the exception of the reticular nucleus which contained neither mu binding sites or mRNA expression, although mu receptor immunoreactivity was found in this nucleus (Delfs, et al., 1994a; Mansour, et al., 1995b; Mansour, et al., 1994; Tempel & Zukin, 1987). This would indicate that the fibers coursing the reticular nucleus contain mu receptor but it does not explain why binding was not seen in the rat. The lack of mu receptor mRNA could possibly be explained by the lack of mu receptor containing perikarya in the reticular nucleus of the rat. Also in contrast to the adult rat, the fetal monkey was found to contain mu binding sites in many nuclei of the hypothalamus including the supraoptic, arcuate, paraventricular and dorsomedial nuclei and the lateral hypothalamus, all of which contain mu receptor mRNA in the fetal monkey, although low binding densities were found in the latter two hypothalamic nuclei of the rat (Mansour, et al., 1988). The medial habenula contains distinct mu receptor binding sites and mu receptor mRNA in the fetal monkey. The habenula sends afferent projections to the

interpeduncular nucleus via the fasciculus retroflexus and interestingly, all contain mu receptor binding sites. This same pattern is found in the adult rat which also contain mu receptor immunoreactivity in the medial habenula, fasciculus retroflexus and the interpeduncular nucleus(Mansour, et al., 1995b).

Mu receptor binding in the fetal monkey was quite similar when comparing the day 70 and day 150 fetal monkeys. The main difference was the amount of binding density present within specific nuclei. One of the most striking differences was seen in the paraventricular nucleus of the thalamus in which the 150 day fetal monkey had densities approximately three times that of the day 70 fetal monkey. The paraventricular nucleus projects to the prefrontal cortex which is associated, in part, with higher intelligence and behavior and to the limbic cortex, amygdala and ventral striatum. It also receives afferents projections from the hypothalamus, amygdala, nucleus of the solitary tract, periaqueductal gray, parabrachial, raphe, and locus coeruleus. Mu receptor could be acting to modulate physiological and emotional reactions to alarm, fear, anxiety or panic and the accompanying analgesia which is associated with these situations. It could be argued that this increase in mu receptor binding density is simply due to the increased size of the fetal brain at 150 days of gestation yet other nuclei throughout the brain such as the striatum, reticular nucleus of the thalamus, periaqueductal gray and the spinal trigeminal nucleus all have comparable levels of mu receptor binding densities in both the day 70 and day 150 fetal monkeys.

The distribution of mu receptor in the fetal monkey brain as evidenced by mu receptor mRNA localization and mu receptor binding indicates that mu receptor is present early in gestation and in the limbic, sensory, and motor systems of the fetal monkey brain and could actively participate, albeit in an inhibitory capacity, in the modulation of the neural circuitry critical for survival after birth. Future areas of research would encompass the effects that drugs of abuse have on the ontogeny of the mu receptor and the behavioral consequences thereof. With the recent cloning of rhesus monkeys, it would be feasible to

utilize this model to delineate the effects cocaine or morphine on the development of the mu receptor in the brain while eliminating the genetic variability that normally exists between animals.

References

Altman, J., & Bayer, S. A. (1988a). Development of the rat thalamus: I. Mosaic organization of the thalamic neuroepithelium. Journal of Comparative Neurology, 275, 346-377.

Altman, J., & Bayer, S. A. (1988b). Development of the rat thalamus: III. Time and site of origin and settling pattern of neurons of the reticular nucleus. Journal of Comparative Neurology, 275, 406-428.

Arvidsson, R., Reidl, M., Chakrabarti, S., Lee, J.-H., Nakano, A. H., Dado, R. J., Loh, H. H., Law, P.-Y., Wessendorf, M. W., & Elde, R. (1995). Distribution and targeting of a μ -opioid receptor (MOR1) in brain and spinal cord. Journal of Neuroscience, 15(5), 3328-3341.

Atweh, S. F., & Kuhar, M. J. (1977). Autoradiographic localization of opiate receptors in rat brain. I. Spinal cord and lower medulla. Brain Research, 124, 53-67.

Battaglia, G., Lizier, C., Colacitti, C., Princivalle, A., & Spreafico, R. (1994). A reticuloreticular commissural pathway in the rat thalamus. Journal of Comparative Neurology, 347, 127-138.

Bayer, S. A. (1983). ^3H -Thymidine-radiographic studies of neurogenesis in the rat olfactory bulb. Experimental Brain Research, 50, 329-340.

Birnbaumer, L., Abramowitz, J., & Brown, A. M. (1990). Receptor-effector coupling by G proteins. Biochimica et Biophysica Acta, 1031, 163-224.

Blackford, S. P., Little, P. J., & Kuhn, C. M. (1992). μ - and κ -opiate receptor control of prolactin secretion in rats: Ontogeny and interaction with serotonin. Endocrinology, 131, 2891-2897.

Bossy, J. (1980). Development of olfactory and related structures in staged human embryos. Anatomy and Embryology, 161, 225-236.

Brand, S., & Rakic, P. (1979). Genesis of the primate neostriatum: [³H]Thymidine autoradiographic analysis of the time of neuron origin in the rhesus monkey. Neuroscience, 4, 767-778.

Brand, S., & Rakic, P. (1980). Neurogenesis of the nucleus accumbens septi and neighboring septal nuclei in the rhesus monkey: A combined [³H]thymidine and electron microscopic study. Neuroscience, 5, 2125-2138.

Bunzow, J. R., Zhang, G., Bouvier, C., Saez, C., Ronnekleiv, O. K., Kelly, M. J., & Grandy, D. K. (1995). Characterization and distribution of a cloned rat μ -opioid receptor. Journal of Neurochemistry, 64, 14-24.

Chabot, J.-G., Tong, Y., Shen, S.-H., O'Dowd, B. F., George, S. R., & Quirion, R. (1995). Ontogeny of the expression of the mu opioid receptor gene in rat brain: An *in situ* hybridization study. Abstract (534.13). In Society for Neuroscience, 21, Part 2 (pp. 1357). San Diego, CA:

Chen, W. P., Witkin, J. W., & Silverman, A. J. (1989). β -endorphin and gonadotropin-releasing hormone synaptic input to gonadotropin-releasing hormone neurosecretory cells in the male rat. Journal of Comparative Neurology, 286, 85-95.

Chen, Y., Mestek, A., Liu, J., Hurley, J. A., & Yu, L. (1993). Molecular cloning and functional expression of a mu opioid receptor from rat brain. Molecular Pharmacology, 44, 8-12.

Childers, S. R. (1991). Opioid receptor-coupled second messenger systems. Life Sciences, 48, 1991-2003.

Chiriboga, C. A. (1993). Neurologic complications of drug and alcohol abuse: Fetal effects. Neurologic Clinics, 11(3), 707-728.

Chowen, J. A., Steiner, R. A., & Clifton, D. K. (1991). Semiquantitative analysis of cellular somatostatin mRNA levels by in situ hybridization histochemistry. In P. M. Conn (Ed.), Methods in Neurosciences: Neuropeptide technology; gene expression and neuropeptide receptors. (pp. 137-158). San Diego: Academic Press.

Civelli, O., Birnberg, N., & Herbert, E. (1982). Detection and quantitation of pro-opiomelanocortin mRNA in pituitary and brain tissues from different species. Journal of Biological Chemistry, 257, 6783-6787.

Clifford, D. B. (1984). Chapter 5: The Somatosensory System and Pain. In A. L. Pearlman & R. C. Collins (Eds.), Neurological Pathophysiology (pp. 74-85). New York: Oxford University Press.

Cornwall, J., Cooper, J. D., & Phillipson, O. T. (1990). Projections to the rostral reticular thalamic nucleus in the rat. Experimental Brain Research, 80, 157-171.

Cuthbert, B. N., Holaday, J. W., Meyerhoff, J., & Li, C. H. (1989). Intravenous beta-endorphin: Behavioral and physiological effects in conscious monkeys. Peptides, 10, 729-734.

Da Costa Gomez, T. M., & Behbehani, M. M. (1995). An electrophysiological characterization of the projection from the central nucleus of the amygdala to the periaqueductal gray of the rat: the role of opioid receptors. Brain Research, 689, 21-31.

Delfs, J. M., Kong, H., Mestek, A., Chen, Y., Yu, L., Reisine, T., & Chesselet, M.-F. (1994a). Expression of mu opioid receptor mRNA in rat brain: An in situ hybridization study at the single cell level. Journal of Comparative Neurology, 345, 46-68.

Delfs, J. M., Yu, L., Ellison, G. D., Reisine, T., & Chesselet, M.-F. (1994b). Regulation of μ -opioid receptor mRNA in rat globus pallidus: Effects of enkephalin increases induced by short- and long-term haloperidol administration. Journal of Neurochemistry, 63, 777-780.

Duman, R. S., Tallman, J. F., & Nestler, E. J. (1988). Acute and chronic opiate-regulation of adenylate cyclase in brain: Specific effects in locus coeruleus. Journal of Pharmacology and Experimental Therapeutics, 246(3), 1033-1039.

Edley, S. M., & Herkenham, M. (1984). Comparative development of striatal opiate receptors and dopamine revealed by autoradiography and histofluorescence. Brain Research, 305, 27-42.

Elkabes, S., Loh, Y. P., Nieburgs, A., & Wray, S. (1989). Prenatal ontogenesis of pro-opiomelanocortin in the mouse central nervous system and pituitary gland: an *in situ* hybridization and immunocytochemical study. Developmental Brain Research, 46, 85-95.

Ferin, M. (1989). The role of endogeneous opioid peptides in the regulation of the menstrual cycle. Journal of Steroid Biochemistry, 33(4B), 683-685.

Ferin, M. (1993). Neuropeptides, the stress response, and the hypothalamo-pituitary-gonadal axis in the female rhesus monkey. Annals of the New York Academy of Sciences, 697, 106-116.

Fields, H. L., Heinricher, M. M., & Mason, P. (1991). Neurotransmitters in nociceptive modulatory circuits. Annual Review of Neuroscience, 14, 219-245.

Foley, K. M. (1993). Opioids. Neurological Complications of Drug and Alcohol Abuse, 11(3), 503-522.

Franck, L., & Vilaridi, J. (1995). Assessment and management of opioid withdrawal in ill neonates. Neonatal Network, 14(2), 39-48.

Gee, C. E., Chen, C.-L. C., Roberts, J. L., Thompson, R., & Watson, S. J. (1983). Identification of proopiomelanocortin neurones in rat hypothalamus by *in situ* cDNA-mRNA hybridization. Nature, 306, 374-376.

Gerfen, C. R. (1992). The neostriatal mosaic: Multiple levels of compartmental organization in the basal ganglia. Annual Review of Neuroscience, 15, 285-320.

Gerfen, C. R., & Wilson, C. J. (1996). The basal ganglia. In L. W. Swanson, A. Bjorklund, & T. Hokfelt (Eds.), Handbook of Chemical Neuroanatomy, Vol. 12: Integrated Systems of the CNS, Part III (pp. 371-468). New York: Elsevier Science.

Goldstein, A., & Naidu, A. (1989). Multiple opioid receptors: Ligand selectivity profiles and binding site signatures. Molecular Pharmacology, 36, 265-272.

Gong, Q., & Shipley, M. T. (1995). Evidence that pioneer olfactory axons regulate telencephalon cell cycle kinetics to induce the formation of the olfactory bulb. Neuron, 14, 91-101.

Gribnau, A. A. M., & Geijsberts, L. G. M. (1981). Developmental stages in the rhesus monkey (*Macaca mulatta*). Advances in Anatomy Embryology and Cell Biology, 68, 1-84.

Gribnau, A. A. M., & Geijsberts, L. G. M. (1985). Morphogenesis of the brain in staged rhesus monkey embryos. Advances in Anatomy Embryology and Cell Biology, 91, 1-69.

Handa, B. K., Lane, A. C., Lord, J. A. H., Morgan, B. A., Rance, M. J., & Smith, C. F. C. (1981). Analogues of β -LPH₆₁₋₆₄ possessing selective agonist activity at μ -opiate receptors. European Journal of Pharmacology, 70, 531-540.

Harris, H. W., & Nestler, E. J. (1993). Opiate regulation of signal-transduction pathways. In R. P. Hammer Jr. (Ed.), The Neurobiology of Opiates (pp. 301-332). Boca Raton: CRC Press.

Hauser, K. F., McLaughlin, P. J., & Zagon, I. S. (1989). Endogenous opioid systems and the regulation of dendritic growth and spine formation. Journal of Comparative Neurology, 281, 13-22.

Hess, D. L., Spies, H. G., & Hendricks, A. G. (1981). Diurnal steroid patterns during gestation in the rhesus macaque: Onset, daily variation, and the effects of dexamethasone treatment. Biology of Reproduction, 24, 609-616.

Hiller, J. M., Pearson, J., & Simon, E. J. (1973). Distribution of stereospecific binding of the potent narcotic analgesic etorphine in the human brain: Predominance in the limbic system. Research Communications in Chemical Pathology and Pharmacology, 6, 1052-1062.

Honda, C. N., & Arvidsson, U. (1995). Immunohistochemical localization of delta- and mu-opioid receptors in primate spinal cord. NeuroReport, 6, 1025-1028.

Hughes, J., Smith, T. W., Kosterlitz, H. W., Fothergill, L. A., Morgan, B. A., & Morris, H. R. (1975). Identification of two related pentapeptides from the brain with potent opiate agonist activity. Nature, 258, 577-579.

Ilinsky, I. A., & Kultas-Ilinsky, K. (1995). Chapter 19: The basal ganglia and the thalamus. In P. M. Conn (Ed.), Neuroscience in Medicine (pp. 343-368). Philadelphia: J. B. Lippincott Company.

Jones, E. G. (1975). Some aspects of the organization of the thalamic reticular complex. Journal of Comparative Neurology, 162, 285-308.

Kalil, K. (1978). Patch-like termination of thalamic fibers in the putamen of the rhesus monkey: an autoradiographic study. Brain Research, 140, 333-339.

Kalyuzhny, A. E., Arvidsson, U., Wu, W., & Wessendorf, M. W. (1996). μ -Opioid and δ -opioid receptors are expressed in brainstem antinociceptive circuits: Studies using immunocytochemistry and retrograde tract-tracing. Journal of Neuroscience, 16, 6490-6503.

Kelly, M. J., Loose, M. D., & Ronnekleiv, O. K. (1992). Estrogen suppresses mu-opioid and GABA-B mediated hyperpolarization of hypothalamic arcuate neurons. Journal of Neuroendocrinology, 12, 2745-2750.

Kent, J. L., Pert, C. B., & Herkenham, M. (1982). Ontogeny of opiate receptors in rat forebrain: Visualization by in vitro autoradiography. Developmental Brain Research, 2, 487-504.

Khachaturian, H., Lewis, M. E., Alessi, N. E., & Watson, S. J. (1985). Time of origin of opioid peptide-containing neurons in the rat hypothalamus. Journal of Comparative Neurology, 236, 538-546.

Khachaturian, H., Lewis, M. E., Haber, S. N., Akil, H., & Watson, S. J. (1984). Proopiomelanocortin peptide immunocytochemistry in rhesus monkey brain. Brain Research Bulletin, 13, 785-800.

Kinney, H. C., Ottoson, C. K., & White, W. F. (1990). Three-dimensional distribution of ^3H -naloxone binding to opiate receptors in the human fetal and infant brainstem. Journal of Comparative Neurology, 291, 55-78.

Kolmac, C. I., & Mitrofanis, J. (1997). Organization of the reticular thalamic projection to the intralaminar and midline nuclei in rats. Journal of Comparative Neurology, 377, 165-178.

Kordower, J. H., Piccinski, P., & Rakic, P. (1992). Neurogenesis of the amygdaloid nuclear complex in the Rhesus monkey. Developmental Brain Research, 68, 9-15.

Kordower, J. H., & Rakic, P. (1990). Neurogenesis of the magnocellular basal forebrain nuclei in the rhesus monkey. Journal of Comparative Neurology, 291, 637-653.

Kraus, J., Horn, G., Simprich, A., Simon, T., Mayer, P., & Holtt, V. (1995). Molecular cloning and functional analysis of the rat μ opioid receptor gene promoter. Biochemical and Biophysical Research Communications, 215, 591-597.

Kuhar, M. J., Pert, C. B., & Snyder, S. H. (1973). Regional distribution of opiate receptor binding in monkey and human brain. Nature, 245, 447-450.

Lamotte, C., Pert, C. B., & Snyder, S. H. (1976). Opiate receptor binding in primate spinal cord: Distribution and changes after dorsal root section. Brain Research, 112, 407-412.

Lauder, J. M. (1995). Chapter 8: Neuroembryology and Differentiation. In P. M. Conn (Ed.), Neuroscience in Medicine (pp. 137-149). Philadelphia: J.B. Lippincott Company.

Laurent-Huck, F. M., Anguelova, E., Rene, F., Stoeckel, M. E., & Felix, J. M. (1993). Ontogeny of prodynorphin gene expression in the rat hypothalamus. Developmental Brain Research, 75, 45-53.

Levitt, P., & Rakic, P. (1982). The time of genesis, embryonic origin and differentiation of the brain stem monoamine neurons in the rhesus monkey. Developmental Brain Research, 4, 35-57.

Lewis, M. E., Khachaturian, H., Akil, H., & Watson, S. J. (1984). Anatomical relationship between opioid peptides and receptors in rhesus monkey brain. Brain Research Bulletin, 13, 801-812.

Li, C. H., & Chung, D. (1976). Isolation and structure of an untriakontapeptide with opiate activity from camel pituitary glands. Proceedings of the National Academy of Sciences USA, 73, 1145-1148.

Lidow, M. S., & Rakic, P. (1995). Neurotransmitter receptors in the proliferative zones of the developing primate occipital lobe. Journal of Comparative Neurology, 360, 393-402.

Loh, H. H., Tseng, L. F., Wei, E., & Li, C. H. (1976). β -endorphin is a potent analgesic agent. Proceedings of the National Academy of Sciences USA, 73, 2895-2898.

Loose, M. D., & Kelly, M. J. (1990). Opioids act at μ -receptors to hyperpolarize arcuate neurons via an inwardly rectifying potassium conductance. Brain Research, 513, 15-23.

Lozsadi, D. A. (1994). Organization of cortical afferents to the rostral, limbic sector of the rat thalamic reticular nucleus. Journal of Comparative Neurology, 341, 520-533.

Lozsadi, D. A. (1995). Organization of connections between the thalamic reticular and the anterior thalamic nuclei in the rat. Journal of Comparative Neurology, 358, 233-246.

Mansour, A., Fox, C. A., Akil, H., & Watson, S. J. (1995a). Opioid-receptor mRNA expression in the rat CNS: anatomical and functional implications. Trends in Neuroscience, 18, 22-29.

Mansour, A., Fox, C. A., Burke, S., Akil, H., & Watson, S. J. (1995b). Immunohistochemical localization of the cloned μ opioid receptor in the rat CNS. Journal of Chemical Neuroanatomy, 8, 283-305.

Mansour, A., Fox, C. A., Thompson, R. C., Akil, H., & Watson, S. J. (1994). μ -Opioid receptor mRNA expression in the rat CNS: comparison to μ -receptor binding. Brain Research, 643, 245-265.

Mansour, A., Khachaturian, H., Lewis, M. E., Akil, H., & Watson, S. J. (1988). Anatomy of CNS opioid receptors. Trends in Neuroscience, 11(7), 308-314.

Martin, W. R., Eades, C. G., Thompson, J. A., Huppler, R. E., & Gilbert, P. E. (1976). The effects of morphine- and nalorphine-like drugs in the nondependent and morphine-dependent chronic spinal dog. Journal of Pharmacology and Experimental Therapeutics, 197, 517-532.

McCarley, R. W. (1995). Chapter 29: Sleep, dreams, and states of consciousness. In P. M. Conn (Ed.), Neuroscience in Medicine (pp. 537-553). Philadelphia: J.B. Lippincott Company.

McDowell, J., & Kitchen, I. (1987). Development of opioid systems: peptides, receptors and pharmacology. Brain Research Reviews, 12, 397-421.

McIntosh, T. K., Palter, M., Grasberger, R., Vezina, R., Gerstein, L., Yeston, N., & Egdahl, R. H. (1986). Endorphins in primate hemorrhagic shock: Beneficial actions of opiate antagonists. Journal of Surgical Research, 40, 265-275.

Mestak, A., Hurley, J. H., Bye, L. S., Campbell, A. D., Chen, Y., Tian, M., Liu, J., Schulman, H., & Yu, L. (1995). The human μ opioid receptor: Modulation of functional desensitization by calcium/calmodulin-dependent protein kinase and protein kinase C. Journal of Neuroscience, 15(3), 2396-2406.

Moss, I. R., & Scarpelli, E. M. (1979). Generation and regulation of breathing in utero: Fetal CO₂ response test. Journal of Applied Physiology: Respiration, Environmental, and Exercise Physiology, 47, 527-531.

Nakanishi, S., Inoue, A., Kita, T., Nakamura, M., Chang, A. C. Y., Cohen, S. N., & Numa, S. (1979). Nucleotide sequence of cloned cDNA for bovine corticotropin- β -lipotropin precursor. Nature, 278, 423-427.

Nestler, E. J. (1996). Under Siege: The brain on opiates. Neuron, 16, 897-900.

Netter, F. H. (1986). Nervous System: Part I: Anatomy and Physiology. West Caldwell, New Jersey: CIBA Pharmaceutical Company.

North, R. A., Williams, J. T., Surprenant, A., & Christie, M. J. (1987). μ and δ receptors belong to a family of receptors that are coupled to potassium channels. Proceedings of the National Academy of Sciences USA, 84, 5487-5491.

Ohara, P. T., & Lieberman, A. R. (1985). The thalamic reticular nucleus of the adult rat: experimental anatomical studies. Journal of Neurocytology, 14, 365-411.

Pare, D., & Steriade, M. (1993). The reticular thalamic nucleus projects to the contralateral dorsal thalamus in macaque monkey. Neuroscience Letters, 154, 96-100.

Pasternak, G. W. (1993). Pharmacological mechanisms of opioid analgesics. Clinical Neuropharmacology, 16(1), 1-18.

Pau, K.-Y. F., Berria, M., Hess, D. L., & Spies, H. G. (1996). Opiatergic influence on gonadotropin-releasing hormone and luteinizing hormone release during the macaque menstrual cycle. Biology of Reproduction, 55, 478-484.

Pechnick, R., George, R., & Poland, R. E. (1985). Identification of multiple opiate receptors through neuroendocrine responses. I. Effects of agonists. Journal of Pharmacology and Experimental Therapeutics, 232, 163-169.

Pert, C. B., & Snyder, S. H. (1973). Opiate receptor: Demonstration in nervous tissue. Science, 179, 1011-1014.

Pfeiffer, A., & Herz, A. (1984). Endocrine actions of opioids. Hormones and Metabolic Research, 16, 386-397.

Rakic, P. (1974). Neurons in rhesus monkey visual cortex: Systematic relation between time of origin and eventual disposition. Science, 183, 425-427.

Rakic, P. (1988). Specification of cerebral cortical areas. Science, 241, 170-176.

Rakic, P. (1995). The development of the frontal lobe. Advances in Neurology, 66, 1-5.

Roberts, J. L., Seeburg, P. H., Shine, J., Herbert, E., Baxter, J. D., & Goodman, H. M. (1979). Corticotropin and β -endorphin: Construction and analysis of recombinant DNA complementary to mRNA for the common precursor. Proceedings of the National Academy of Sciences USA, 78, 2153-2157.

Ronnekleiv, O. K., Bosch, M. A., Naylor, B. R., & Kelly, M. J. (1991). Progonadotropin-releasing hormone synthesis and processing: Measurements of mRNA and peptides. Methods in Neuroscience, 5, 85-108.

Ronnekleiv, O. K., Naylor, B. R., Bond, C. T., & Adelman, J. P. (1989). Immunohistochemistry for gonadotropin-releasing hormone (GnRH) and pro-GnRH and in situ hybridization for GnRH messenger ribonucleic acid in rat brain. Molecular Endocrinology, 3, 363-371.

Rius, R. A., Barg, J., Bem, W. T., Coscia, C. J. & Loh, Y. P. (1991). The prenatal developmental profile of expression of opioid peptides and receptors in the mouse brain. Developmental Brain Research, 58, 237-241.

Schmechel, D. E., & Rakic, P. (1979). Arrested proliferation of radial glial cells during midgestation in rhesus monkey. Nature, 277, 303-305.

Schoffelmeer, A. N. M., Wardeh, G., Hogenboom, F., & Mulder, A. H. (1991). β -endorphin: A highly selective endogenous opioid agonist for presynaptic mu opioid receptors. Journal of Pharmacology and Experimental Therapeutics, 258(1), 237-242.

Schofield, B. R., & Cant, N. B. (1997). Ventral nucleus of the lateral lemniscus in guinea pigs: Cytoarchitecture and inputs from the cochlear nucleus. Journal of Comparative Neurology, 379, 363-385.

Seward, E., Hammond, C., & Henderson, G. (1991). μ -Opioid-receptor-mediated inhibition of the N-type calcium-channel current. Proceedings of the Royal Society of London (Series B), 244, 129-135.

Sidman, R. L., & Rakic, P. (1973). Neuronal migration, with special reference to developing human brain: A review. Brain Research, 62, 1-35.

Simon, E. J., Hiller, J. M., & Edelman, I. (1973). Stereospecific binding of the potent narcotic analgesic [3 H]etorphine to rat-brain homogenate. Proceedings of the National Academy of Sciences, USA, 70, 1947-1949.

Smyth, D. G., Massey, D. E., Zakarian, S., & Finnie, M. D. A. (1979). Endorphins are stored in biologically active and inactive forms: Isolation of alpha-N-acetyl peptides. Nature, 279, 252-254.

Spencer, R. F. (1995). Chapter 15: The oculomotor system. In P. M. Conn (Ed.), Neuroscience in Medicine (pp. 249-260). Philadelphia: J.B. Lippincott Company.

Tempel, A., & Zukin, R. S. (1987). Neuroanatomical patterns of the μ , δ , and κ opioid receptors of rat brain as determined by quantitative *in vitro* autoradiography. Proceedings of the National Academy of Sciences, USA, 84, 4308-4312.

Terenius, L. (1973). Stereospecific interaction between narcotic analgesics and a synaptic plasma membrane fraction of rat cerebral cortex. Acta Pharmacologica et Toxicologica, 32, 317-320.

Terenius, L., & Wahlstrom, A. (1974). Inhibitor(s) of narcotic receptor binding in brain extracts and cerebrospinal fluid. Acta Pharmac Tox, Suppl 1, 55, Abstract.

Thompson, R. C., Mansour, A., Akil, H., & Watson, S. J. (1993). Cloning and pharmacological characterization of a rat μ opioid receptor. Neuron, 11, 903-913.

Tranel, D. (1995). Chapter 30: Higher Brain Functions. In P. M. Conn (Ed.), Neuroscience in Medicine (pp. 555-582). Philadelphia: J.B. Lippincott Company.

van der Kooy, D., & Fishel, G. (1987). Neuronal birthdate underlies the development of striatal compartments. Brain Research, 401, 155-161.

van Eerdenburg, F. J. C. M., & Rakic, P. (1994). Early neurogenesis in the anterior hypothalamus of the rhesus monkey. Developmental Brain Research, 79, 290-296.

Wamsley, J. K., Zarbin, M. A., Young III, W. S., & Kuhar, M. J. (1982). Distribution of opiate receptors in the monkey brain: An autoradiographic study. Neuroscience, 7(3), 595-613.

Wang, J. B., Imai, Y., Eppler, C. M., Gregor, P., Spivak, C. E., & Uhl, G. R. (1993). μ opiate receptor: cDNA cloning and expression. Proceedings of the National Academy of Sciences, USA, 90, 10230-10234.

Wardlaw, S. L., Stark, R. I., Baxi, L., & Frantz, A. G. (1979). Plasma β -endorphin and β -lipotropin in the human fetus at delivery: Correlation with arterial pH and pO₂. Journal of Clinical Endocrinology and Metabolism, 49, 888-891.

Wise, S. P., & Herkenham, M. (1982). Opiate receptor distribution in the cerebral cortex of the rhesus monkey. Science, 218, 387-389.

Yaksh, T. L. (1983). *In vivo* studies on spinal opiate receptor systems mediating antinociception. I. Mu and delta receptor profiles in the primate. Journal of Pharmacology and Experimental Therapeutics, 226, 303-316.

Zagon, I. S., & McLaughlin, P. J. (1984). Naltrexone modulates body and brain development in rats: A role for endogenous opioid systems in growth. Life Sciences, 35, 2057-2064.

Zagon, I. S., & McLaughlin, P. J. (1987). Endogenous opioid systems regulate cell proliferation in the developing rat brain. Brain Research, 412, 68-72.

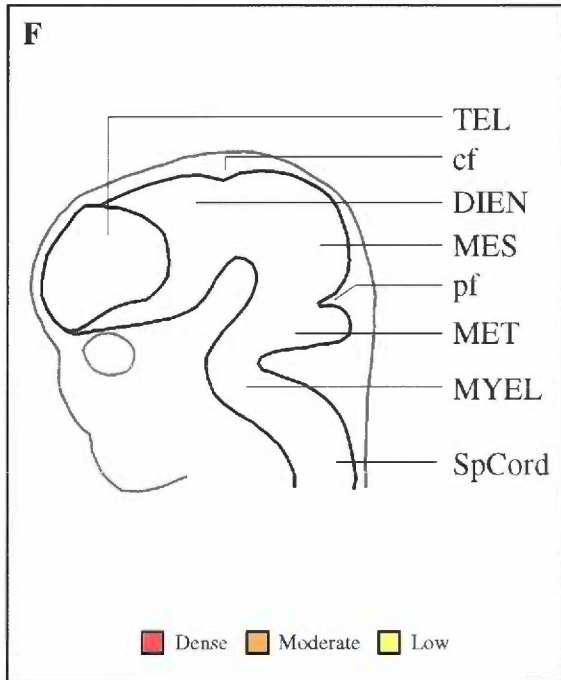
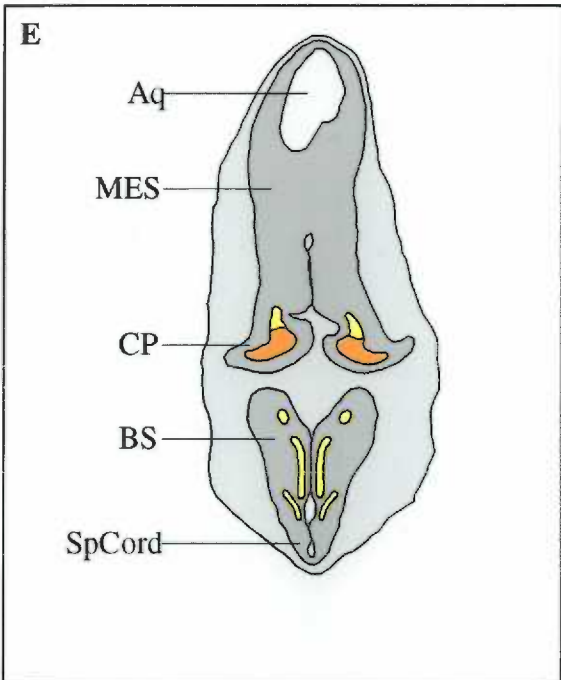
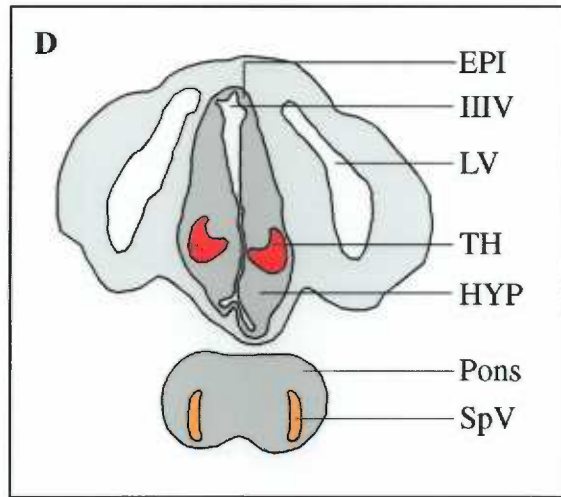
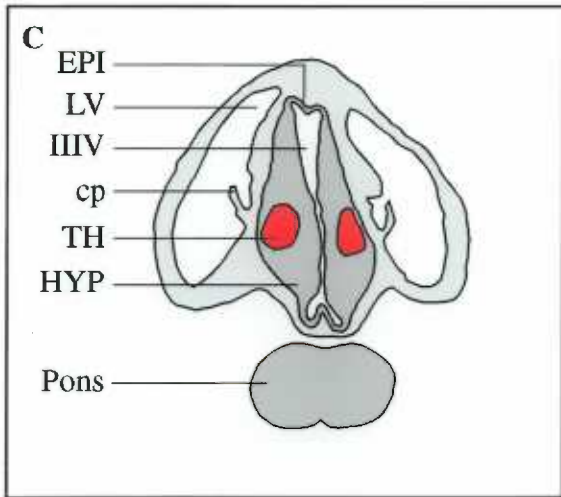
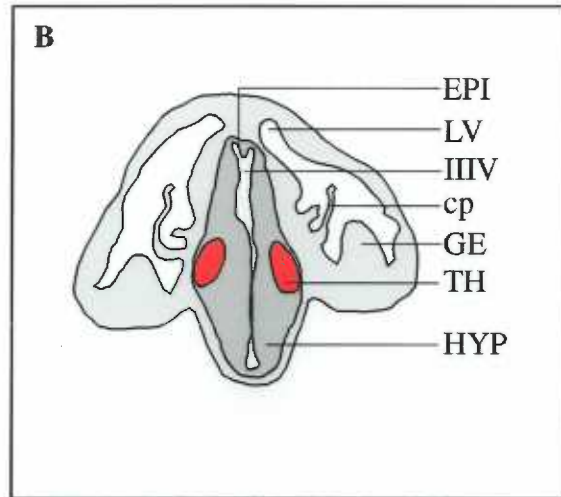
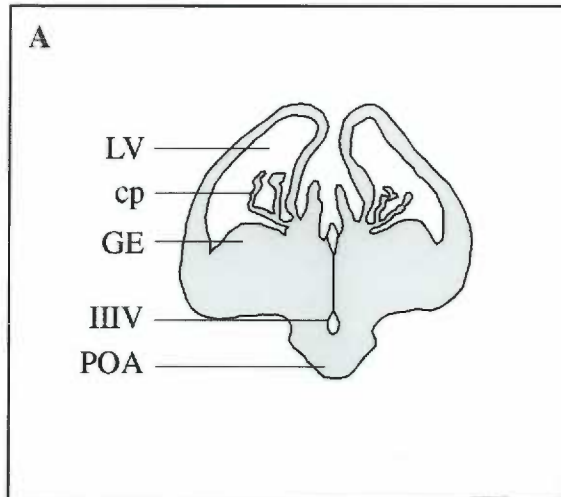
Zagon, I. S., Isayama, T., & McLaughlin, P. J. (1994). Preproenkephalin mRNA expression in the developing and adult rat brain. Molecular Brain Research, 21, 85-98.

Zhu, Y., Anton, B., Hsu, M., Evans, C. J., & Pintar, J. E. (1995). Developmental expression of the mu opioid receptor in the mouse. Abstract 534.12. In Society for Neuroscience, 21 Part 2 (pp. 1357). San Diego, CA.

Zhu, Y., Hsu, M., & Pintar, J. E. (1996). Developmental expression of the mu, kappa, and delta opioid receptors in the mouse. In International Narcotics Research Conference, 27 (pp. 35). Long Beach, CA.

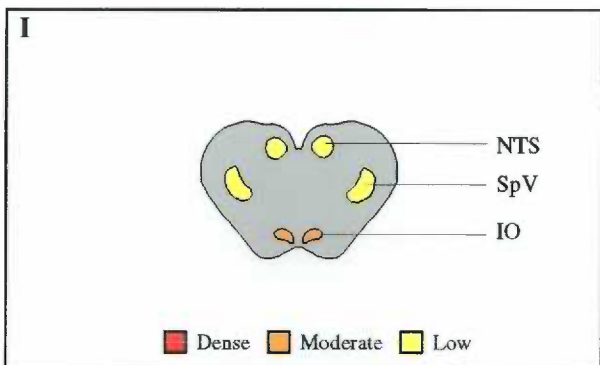
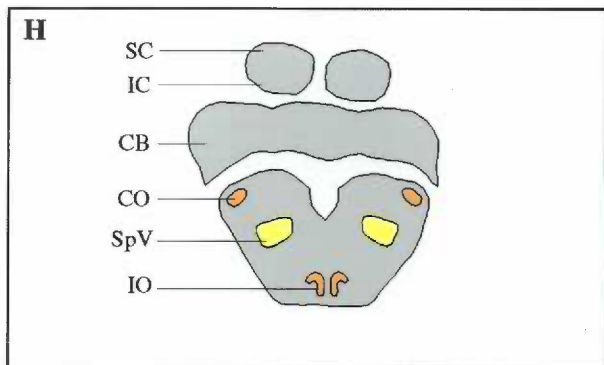
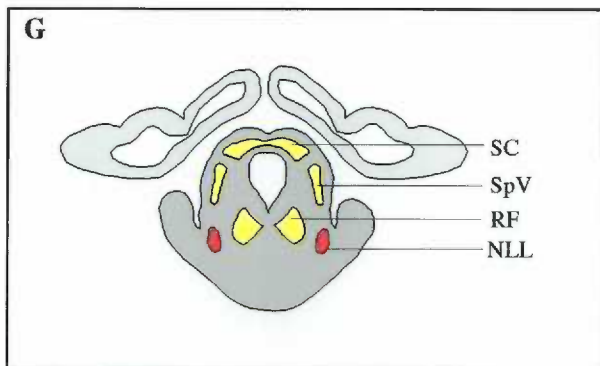
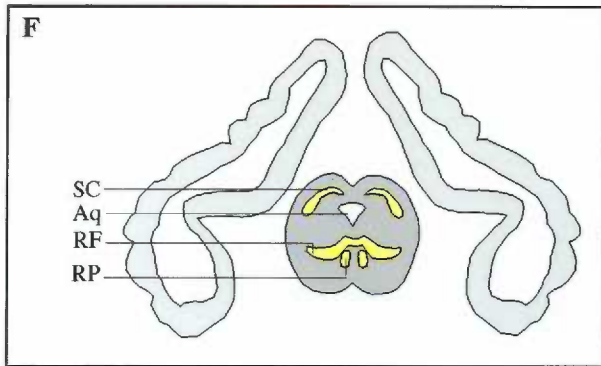
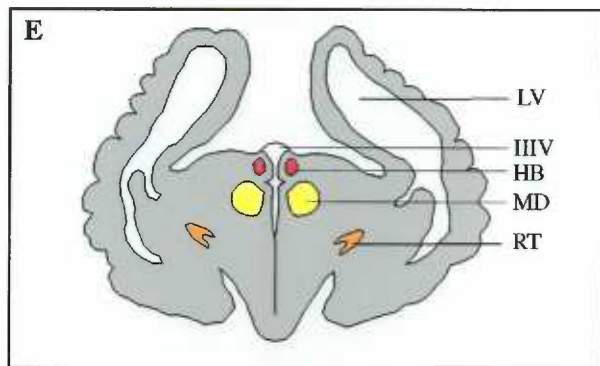
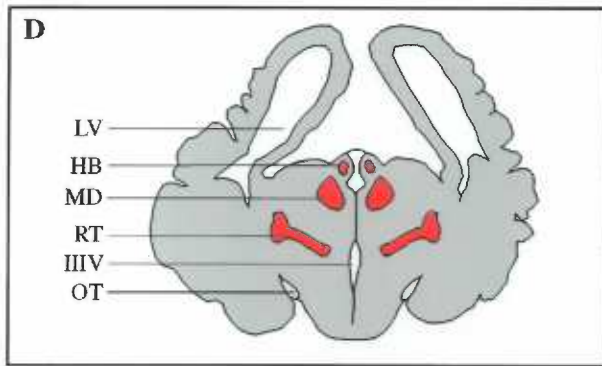
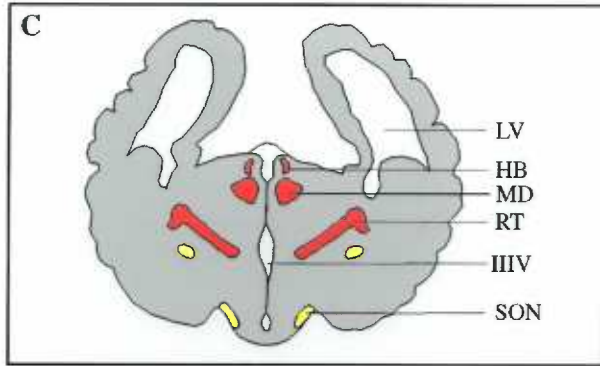
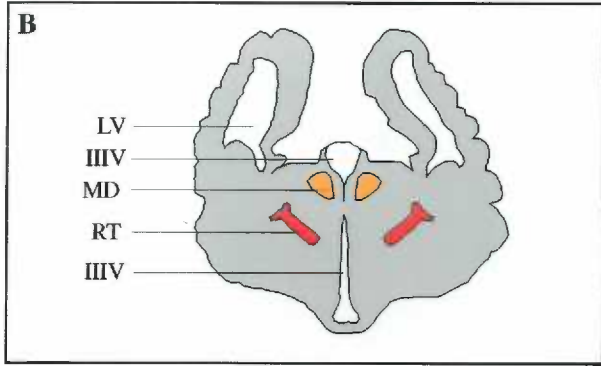
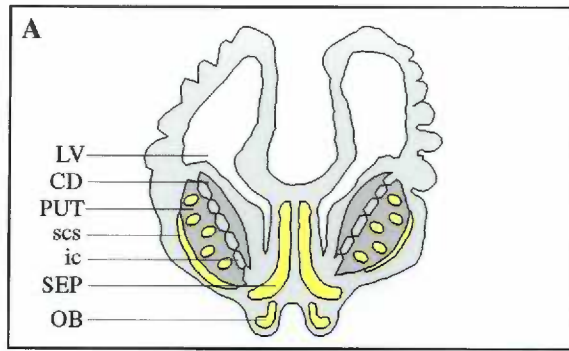
Figures & Tables

Figure 1. Drawings of computer scans of coronal sections from rostral (A) to caudal (E) of day 40 fetal brain showing the morphological development of the brain. The distribution of mu receptor mRNA is illustrated in color: red represents dense, orange represents moderate, yellow represents low levels of autoradiographic grains. A sagittal view of the day 40 brain is also illustrated (F). Abbreviations: Aq, aqueduct; BS, brainstem; cf, cephalic flexure; cp, choroid plexus; CP, cerebellar plates; DIEN, diencephalon; EPI, epithalamus; GE, ganglionic eminence; HYP, hypothalamus; LV, lateral ventricle; MES, mesencephalon; MET, metencephalon; MYEL, myelencephalon; pf, pontine flexure; SpCord, spinal cord; SpV, nucleus of the spinal trigeminal; TEL telencephalon; TH, thalamus; IIIV, third ventricle.



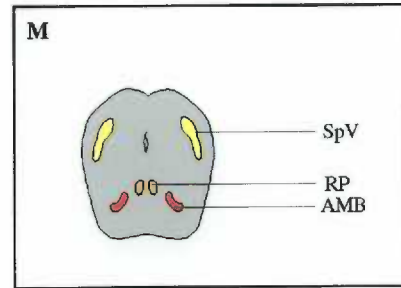
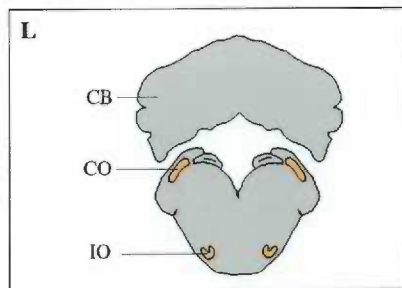
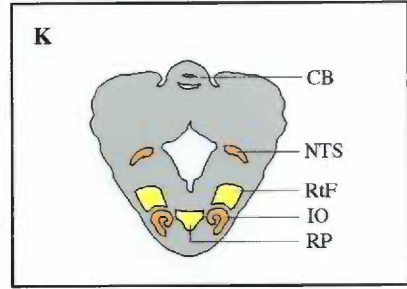
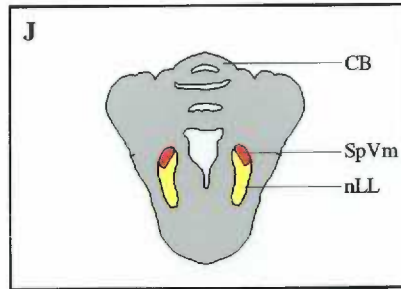
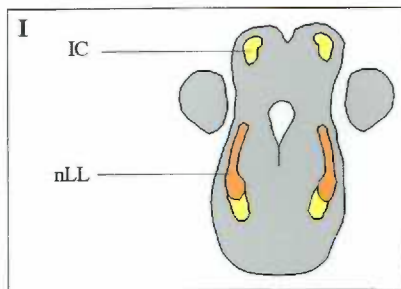
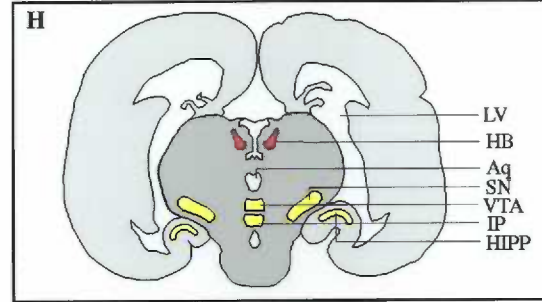
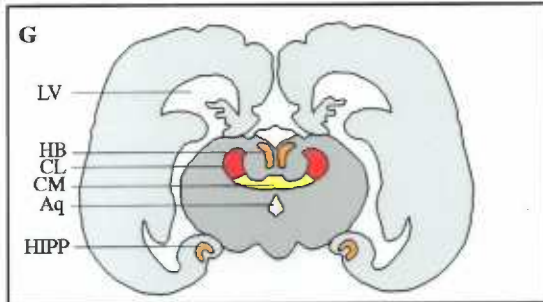
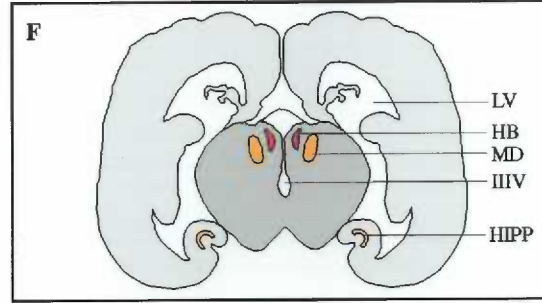
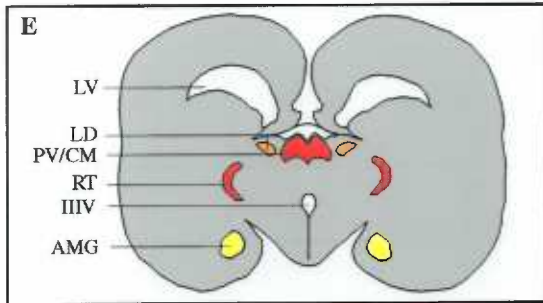
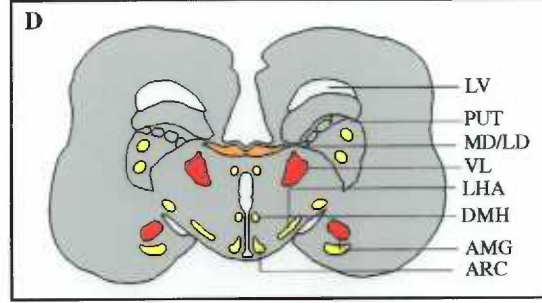
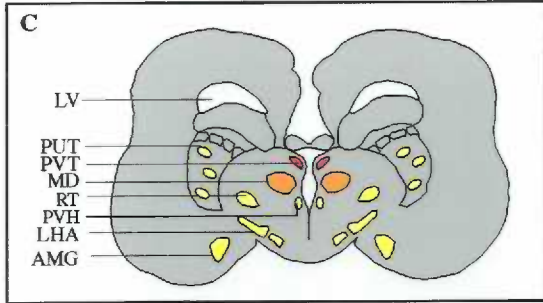
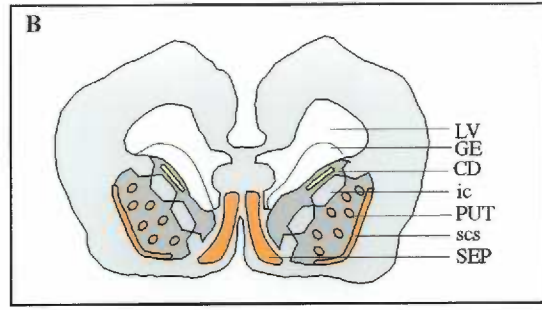
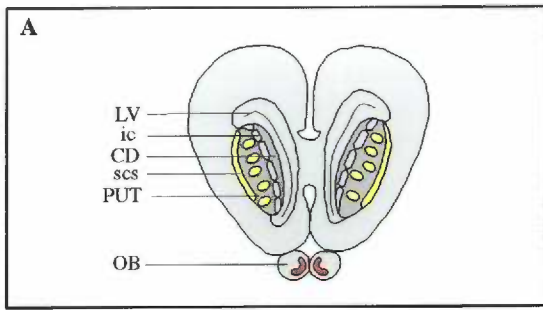
■ Dense ■ Moderate ■ Low

Figure 2. Drawings of computer scans of coronal sections from rostral (A) to caudal (I) of day 60 fetal brain. Each illustration represents a series of sections through the fetal brain from the telencephalon (A), the diencephalon (B-E), mesencephalon (F, G) and the met- and myelencephalon (H, I) showing the relative densities of mu receptor mRNA in situ hybridization signal. The distribution of mu receptor mRNA is illustrated in color, with red representing dense, orange representing moderate, and yellow representing low levels of autoradiographic grains. Abbreviations: AM, anterior medial nucleus of thalamus; Aq, aqueduct; CB, cerebellum; CD, caudate nucleus; CO, cochlear nucleus; HB habenula; ic, internal capsule; IC, inferior colliculus; IO, inferior olivary nucleus; LV, lateral ventricle; MD, mediodorsal nucleus of thalamus; NLL, nucleus of lateral lemniscus; NTS, nucleus of solitary tract; OB, olfactory bulbs; OT, optic tract; PUT, putamen; RF, reticular formation; RP raphe; RT, reticular nucleus of thalamus; SC, superior colliculus; scs subcallosal streak; SEP, septum; SON, supraoptic nucleus of hypothalamus; SpV, spinal trigeminal nucleus; IIIV, third ventricle.



■ Dense ■ Moderate ■ Low

Figure 3. Drawings of computer scans of coronal sections from rostral (A) to caudal (M) of day 70 fetal brain. Each illustration represents a series of coronal sections through the fetal brain from the telencephalon (A,B), diencephalon (C, D, E, F, G), mesencephalon (H, I) and met- and myelencephalon (J, K, L, M) showing the relative densities of mu receptor mRNA in situ hybridization signal. The distribution of mu receptor mRNA is illustrated in color, with red representing dense, orange representing moderate, and yellow representing low levels of autoradiographic grains. Abbreviations: AM, anterior medial nucleus of thalamus; AMB, ambiguous nucleus; AMG, amygdala; Aq, aqueduct; CB, cerebellum; CD, caudate nucleus; CL, centrolateral nucleus of thalamus; CM centromedian nucleus of thalamus; CO, cochlear nucleus; DMH, dorsomedial nucleus of hypothalamus; HB, habenula; HIPPO, hippocampus; ic, internal capsule; IC, inferior colliculus; IO, inferior olivary nucleus; IP, interpeduncular nucleus; LD, laterodorsal nucleus of thalamus; LHA, lateral hypothalamic area; LV, lateral ventricle; MD, mediodorsal nucleus of thalamus; NLL, nucleus of lateral lemniscus; NTS, nucleus of solitary tract; OB olfactory bulbs; OT optic tract; PUT, putamen; PVH, paraventricular nucleus of hypothalamus; PVT, paraventricular nucleus of thalamus; RF, reticular formation; RP, raphe; RT, reticular nucleus of thalamus; SC, superior colliculus; scs, subcallosal streak; SEP, septum; SN, substantia nigra; SON, supraoptic nucleus of hypothalamus; SpV, spinal trigeminal nucleus; VL, ventrolateral nucleus of thalamus; VTA, ventral tegmental area; IIIV, third ventricle.



■ Dense ■ Moderate ■ Low

Figure 4. *in situ* hybridization of mu receptor mRNA antisense probe in coronal sections through the 40 day fetal brain (B-D). A. Representative illustration in sagittal view of the 40 day fetal brain with the vertical lines B, C, D representing the plane of sections shown in figures B, C, D. B. Darkfield photomicrograph showing the distribution of mu receptor mRNA in the ventral thalamus. C. Darkfield photomicrograph illustrating the distribution of mu receptor mRNA in the caudal thalamus and the nucleus of the spinal trigeminal in the pons. D. Darkfield photomicrograph of mu receptor mRNA signal in the developing cerebellar plates and the brainstem. Abbreviations: BS, Brainstem; cp, choroid plexus; CP, cerebellar plates; DIEN, diencephalon; MB, midbrain; TH, thalamus; SpV, nucleus of the spinal trigeminal. Bar = 300 μ m

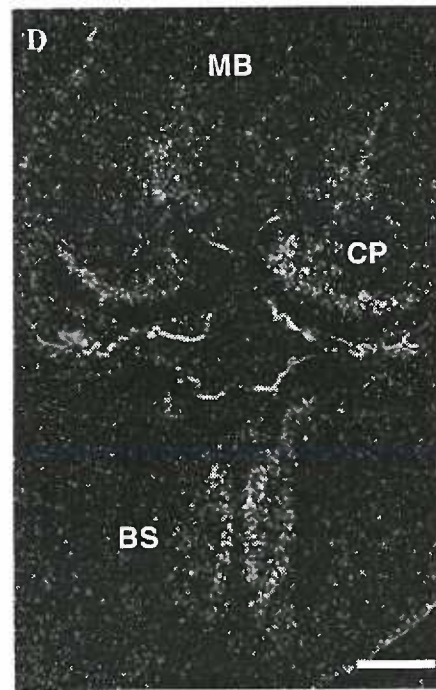
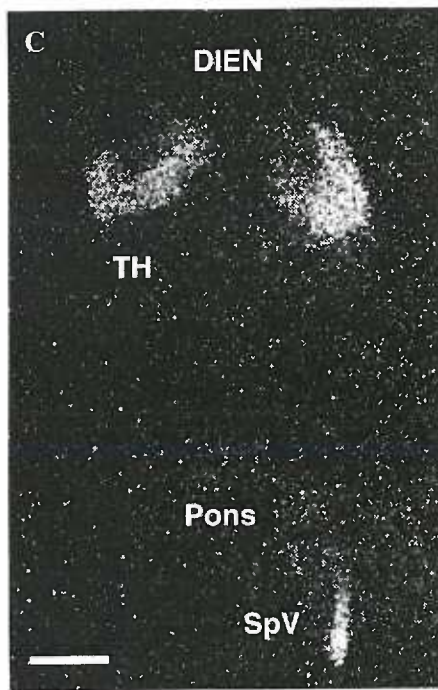
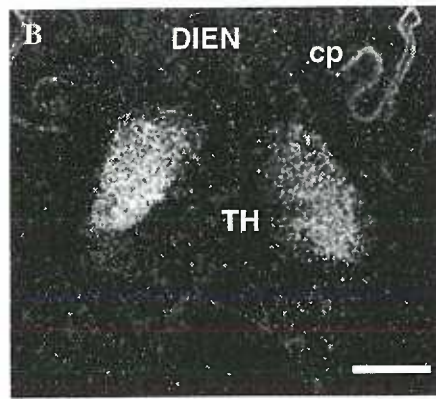
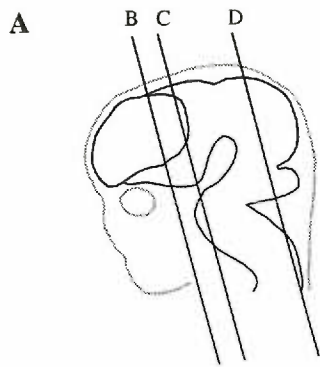


Figure 5. in situ hybridization of mu receptor mRNA in the 40 day fetal monkey. Darkfield (A) and brightfield (B) photomicrographs of coronal sections through the developing diencephalon showing autoradiographic grains indicative of mu receptor mRNA signal in the ventral thalamus. The boxed area in (A) is illustrated in (B). Abbreviations: cp, choroid plexus; DIEN, diencephalon; TH, thalamus. Bar = 300 μ M (A); 60 μ M (B)

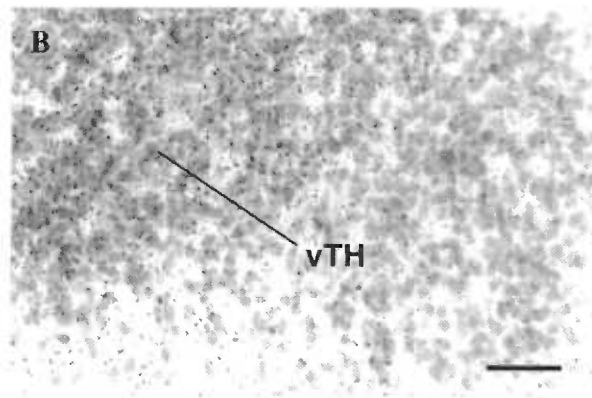
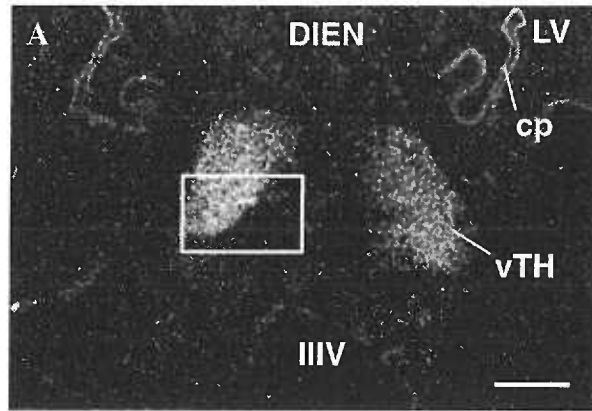


Figure 6. Coronal sections through the rostral forebrain of day 60 fetal monkey which illustrates mu receptor mRNA signal in the olfactory bulbs and septum (A), the putamen (B) and in the habenula, mediodorsal and reticular nuclei of the thalamus (C). Abbreviations: HB, habenula; MD, mediodorsal nucleus of thalamus; OB, olfactory bulbs; PUT, putamen; RT, reticular nucleus of thalamus; scs, subcallosal streak; SEP, septum. Bar = 300 μ m

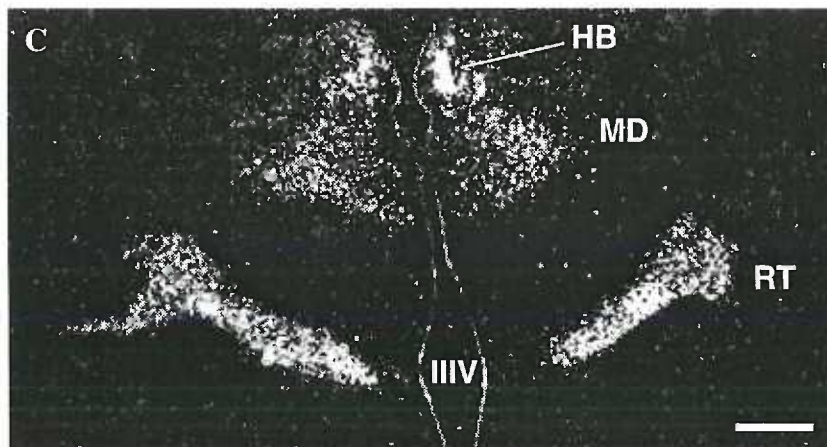
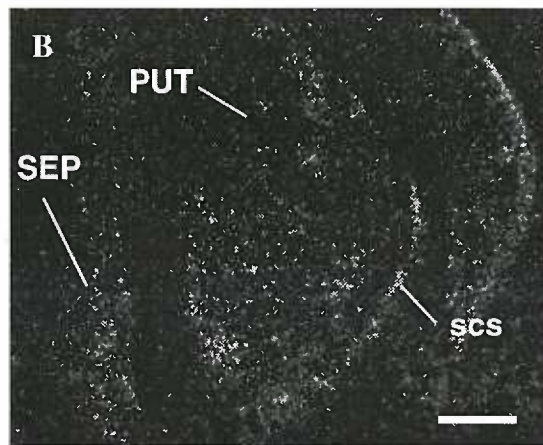
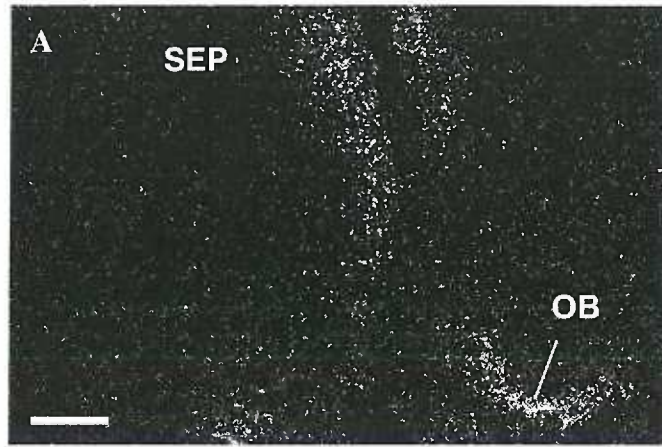


Figure 7. Mu receptor mRNA in situ hybridization in the 70 day fetal monkey. Darkfield photomicrographs of coronal sections through the day 70 fetal brain illustrating mu receptor mRNA in the striatum (A), olfactory bulbs (B), thalamus (C), substantia nigra (D), ventral medial midbrain (E), inferior colliculus and nucleus of the lateral lemniscus (F), raphe nuclei (G), and the rostral spinal trigeminal nucleus (H). Bar = 400 μ m (A), 150 μ m (B), 300 μ m (C, F, G), 75 μ m (D, E, H)

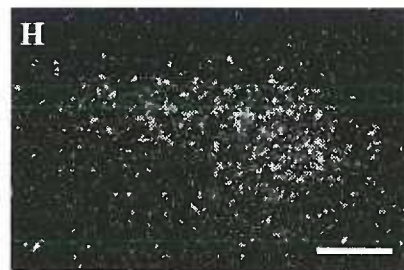
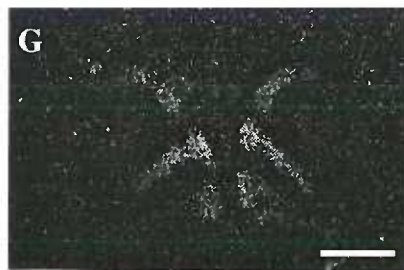
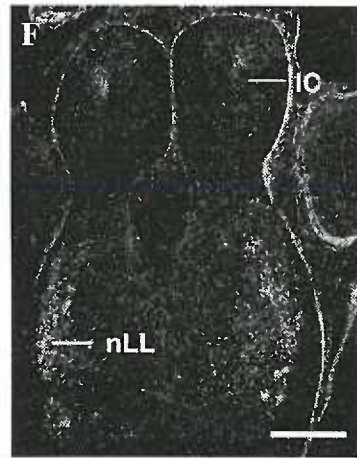
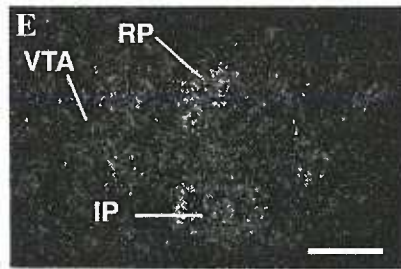
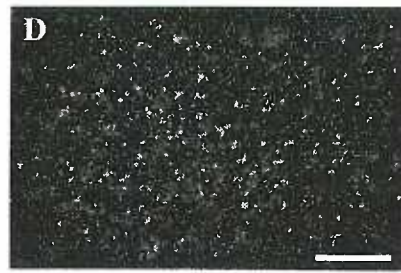
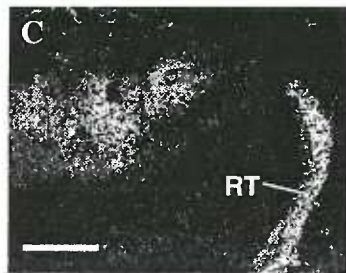
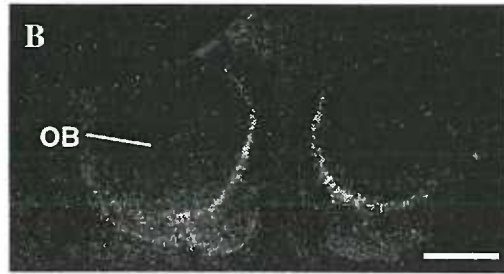


Figure 8. Brightfield and darkfield photomicrographs of the habenula, in the day 60 (A, B) and day 70 (C, D) fetus, which illustrate the distribution of mu receptor mRNA. Bar = 60 μm (A, C), 75 μm (B, D).

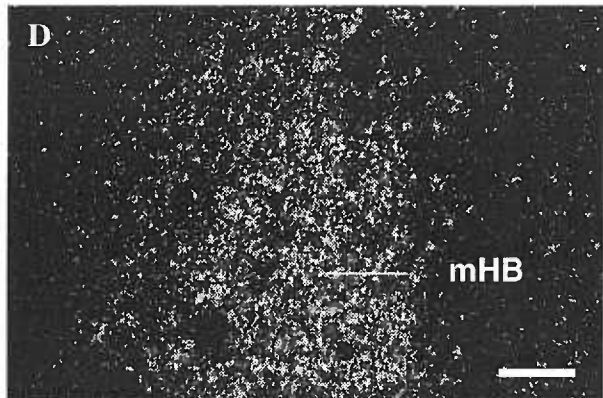
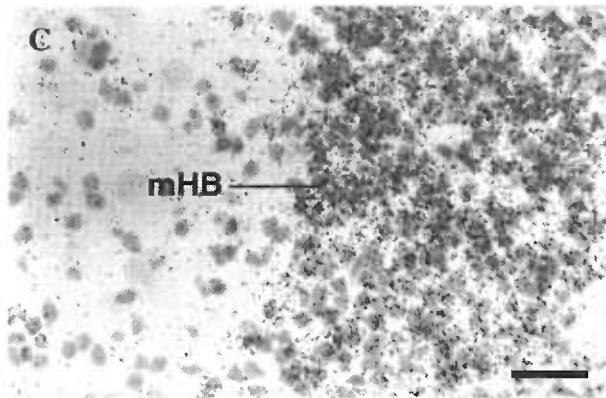
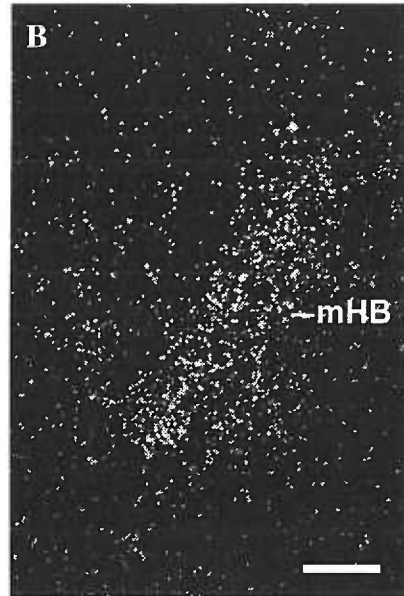
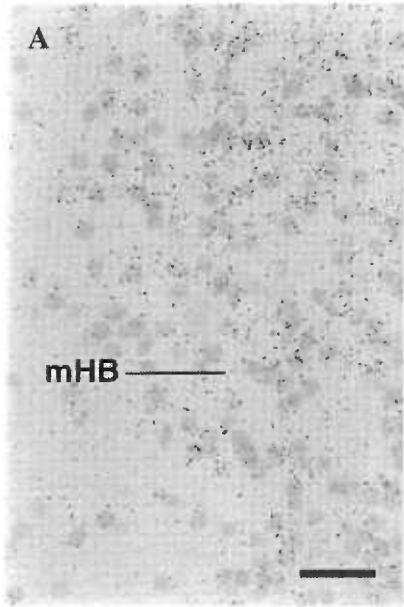


Figure 9. in situ hybridization of mu receptor mRNA.
Brightfield (A, C) and darkfield (B, D) photomicrographs of coronal sections through the nucleus of the lateral lemniscus in the day 60 (A, B) and day 70 (C, D) fetal monkey.
Bar = 60 μm (A, C), 75 μm (B, D).

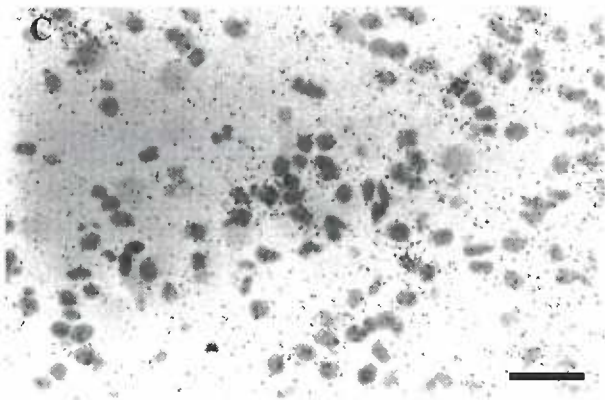
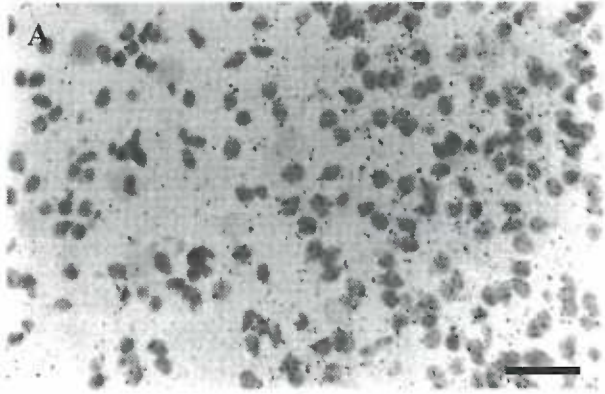


Figure 10. Brightfield (A, C, E) and darkfield (B, D, F) photomicrographs of mu receptor mRNA in situ hybridization signal in the reticular nucleus of the thalamus of the day 60 (A, B), day 70 (C, D) and day 130 (E, F) fetus. Bar = 60 μm (A, C, E), 75 μm (B, D, F).

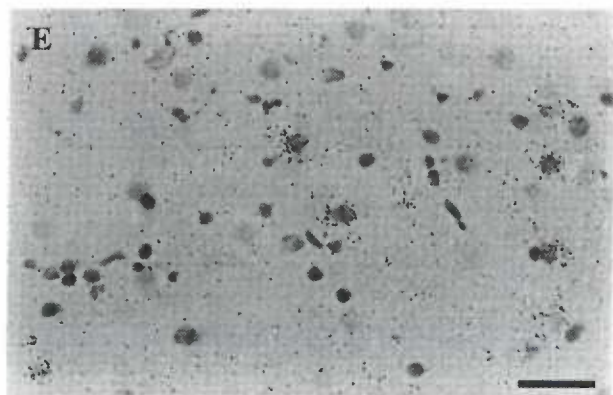
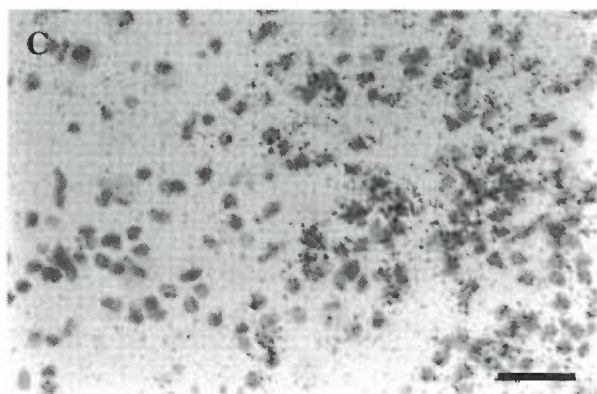
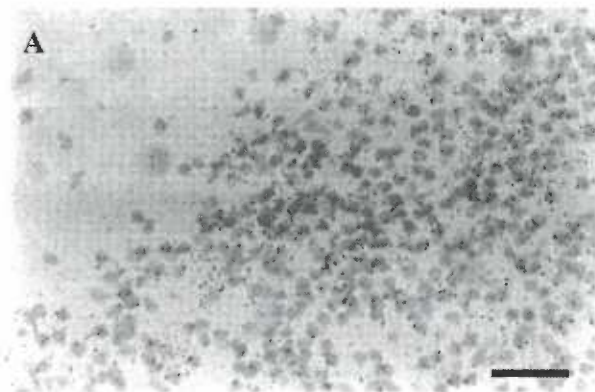


Figure 11. Brightfield (A, C) and darkfield (B, D) photomicrographs of in situ hybridization mu receptor mRNA in the paraventricular nucleus of the thalamus in the day 70 (A, B) and day 130 (C, D) fetus. The boxed area in (B) is illustrated in (A). Note the reduced number of cells per area in the day 130 fetal brain as compared to the day 70 fetus; cell size, as determined using cresyl violet (Nissl stain), however, is about the same. Bar = 60 μm (A, C), 150 μm (B, D).

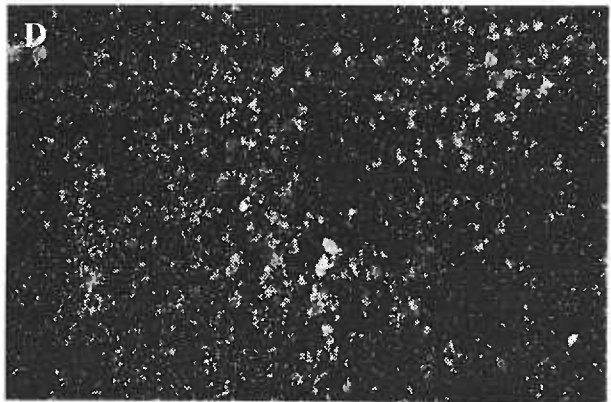
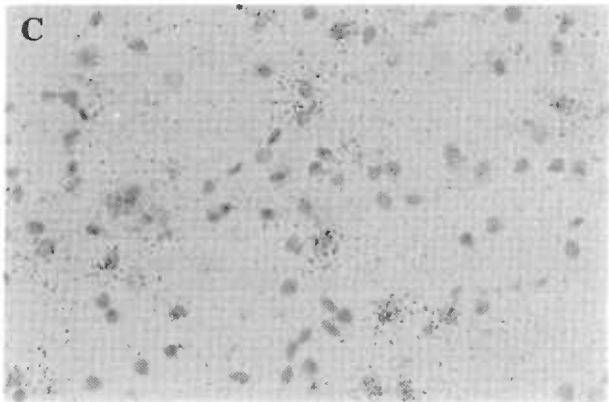
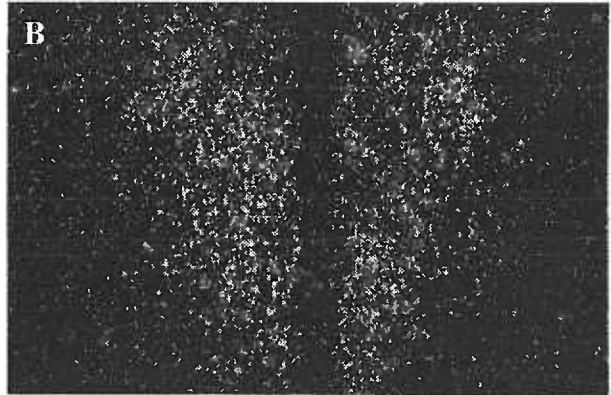
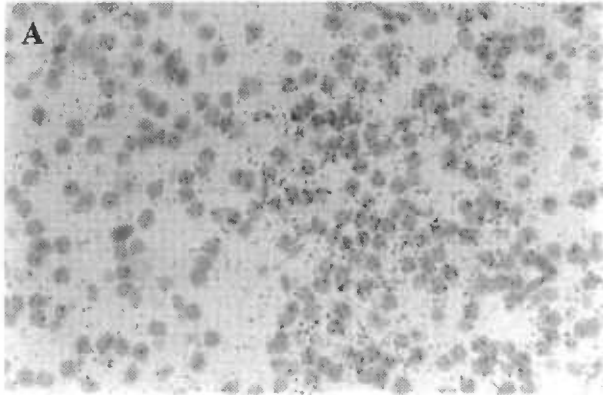


Figure 12. Brightfield (A, C) and darkfield (B, D) photomicrographs of coronal sections through the thalamus of day 70 (A, B) and day 130 (C, D) fetuses which illustrates mu receptor mRNA in situ hybridization signal in the centrolateral nucleus. Bar = 45 μm (A, C), 300 μm (B, D).

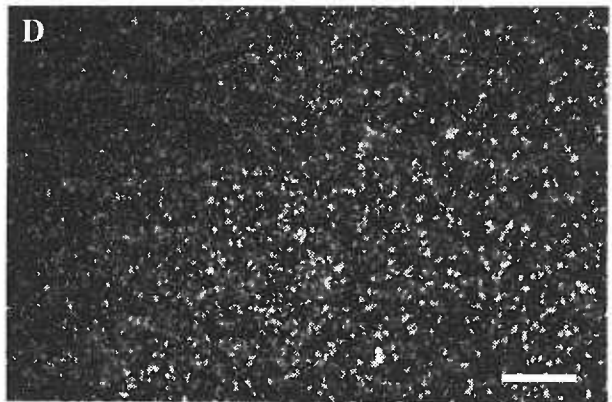
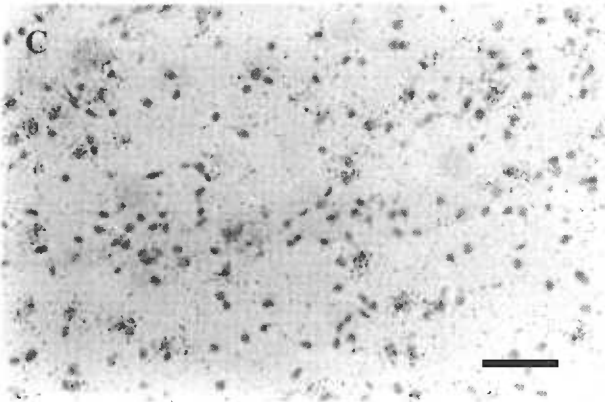
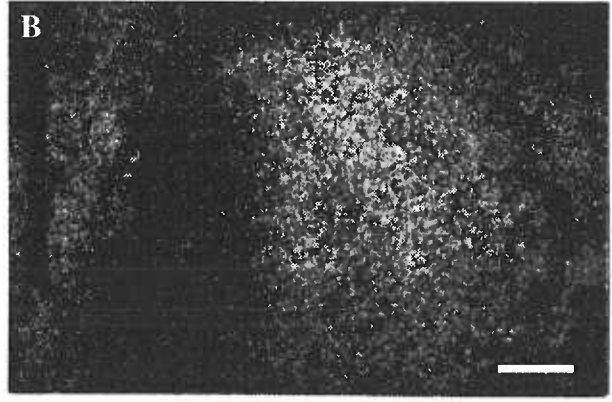
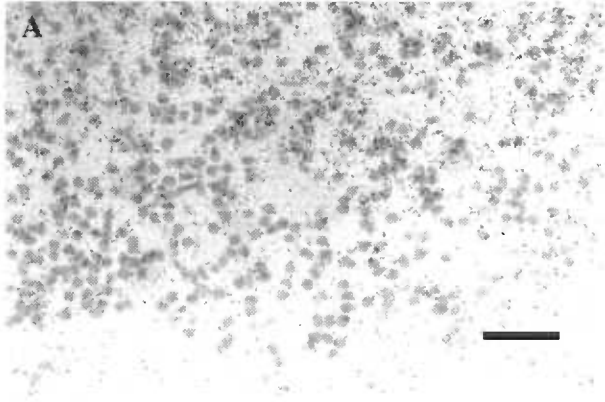


Figure 13. Darkfield views of autoradiograms illustrating the distribution of mu receptor binding in coronal sections from day 70 fetal monkey brain, labeled with [3H] DAMGO. Abbreviations: AMG, amygdala; CB, cerebellum; CD, caudate nucleus; CL, centrolateral nucleus of thalamus; CM centromedian nucleus of thalamus; CO, cochlear nucleus; DTA, dorsal tegmental area; fr, fasciculus retroflexus; HB, habenula; HYP, hypothalamus; IO, inferior olivary nucleus; LV, lateral ventricle; MD, mediodorsal nucleus of thalamus; MG, medial geniculate nucleus of the thalamus; OB olfactory bulbs; OT optic tract; PAG, periaqueductal gray; PUT, putamen; RP, raphe; RT, reticular nucleus of thalamus; SC, superior colliculus; SN, substantia nigra; SpV, spinal trigeminal nucleus. Bar = 2 mm.

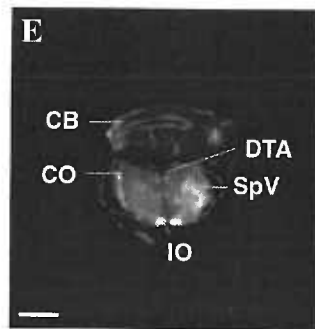
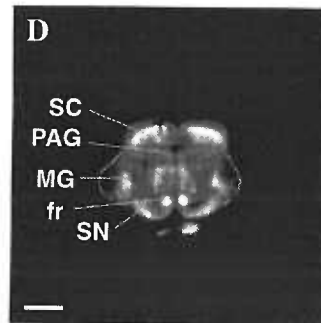
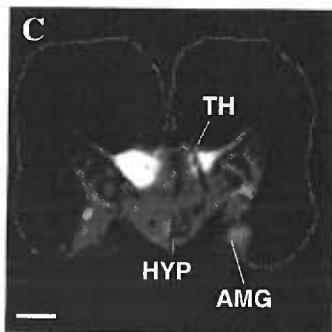
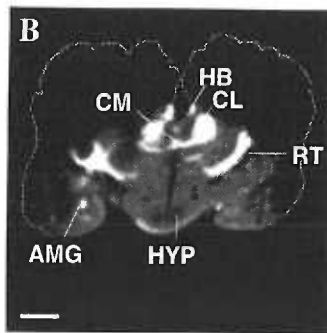
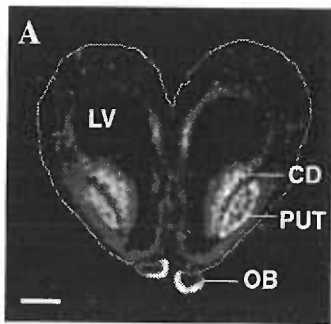


Figure 14. Darkfield views of autoradiograms illustrating the distribution of mu receptor binding in coronal sections from day 150 fetal monkey brain, labeled with [3H] DAMGO. Abbreviations: CB, cerebellum; CD, caudate nucleus; CL, centrolateral nucleus of thalamus; CM, centromedian nucleus of thalamus; CO, cochlear nucleus; fr, fasciculus retroflexus; GPe, external globus pallidus; GPi, internal globus pallidus; HYP, hypothalamus; IC, inferior colliculus; IO, inferior olivary nucleus; IP, interpeduncular nucleus; LD, laterodorsal nucleus of thalamus; MD, mediodorsal nucleus of thalamus; OB, olfactory bulbs; OT, optic tract; PAG, periaqueductal gray; Pn, pontine nuclei; PUT, putamen; PVT, paraventricular nucleus of thalamus; RF, reticular formation; RP, raphe; RT, reticular nucleus of thalamus; SC, superior colliculus; SEP, septum; SN, substantia nigra; SpV, spinal trigeminal nucleus; VL, ventrolateral nucleus of thalamus. Bar = 2 mm.

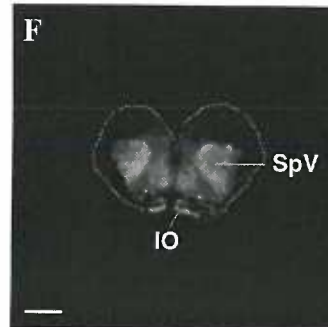
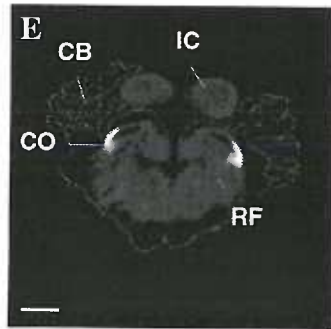
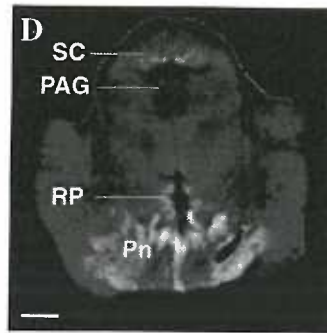
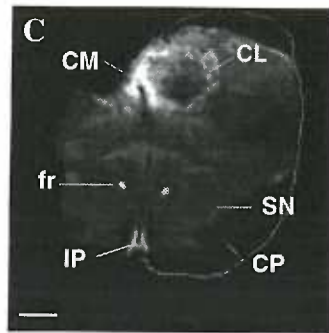
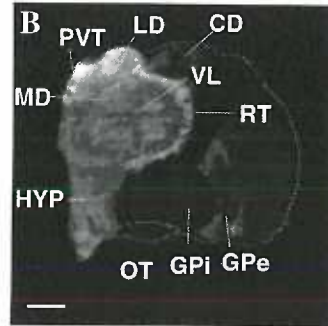
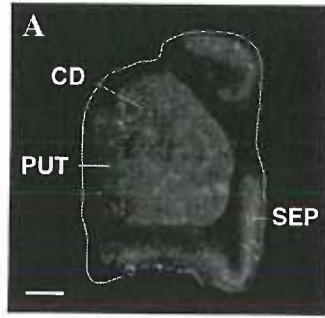


Figure 15. Bar graph illustrating the distribution of mu receptor binding sites in the day 70 (n = 3) and the day 150 (n = 1) fetal monkey brain. Binding densities were measured in nCi per gram of tissue.

Distribution of Mu Receptor Binding Sites in Day 70 and Day 150 Fetal Monkeys

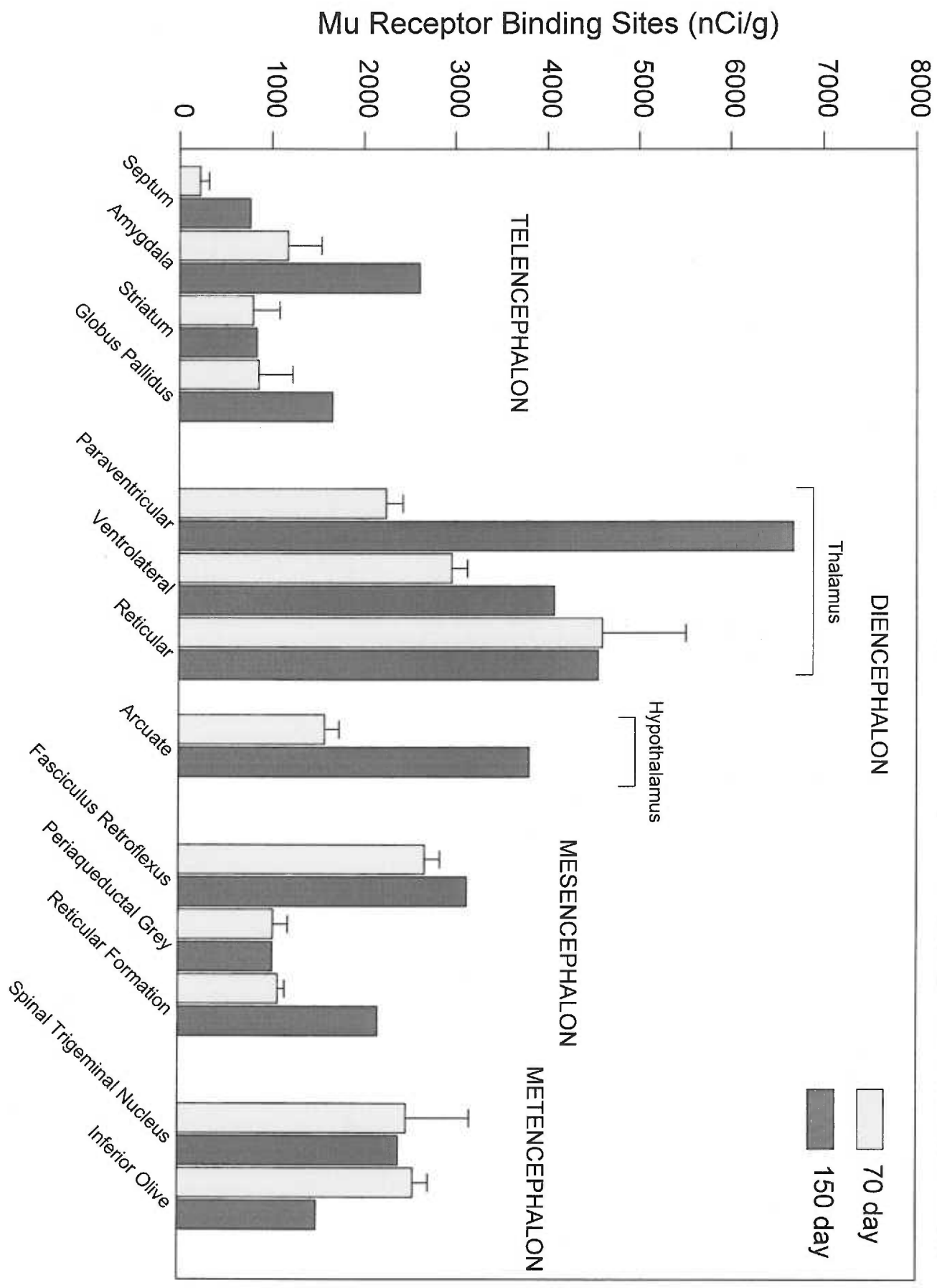


Table I

Body Weight, Crown-Rump Length, Head Circumference and Brain Weight Measurements in the day 40, day 45, day 60, day 70 and day 130 Monkey Fetus

Animal	Sex	Body Weight (g)	Crown-Rump Length (cm)	Head Circumference (cm)	Brain Weight (g)
<u>40d</u>					
M245	-	0.4	1.6	-	-
M246	-	0.8	2.0	2.4	-
<u>45d</u>					
M253	-	1.4	2.2	3.3	-
M256	-	1.0	2.15	2.9	-
<u>60d</u>					
M248	M	10.9	5.2	6.2	-
M249	F	7.3	4.5	5.5	-
<u>70d</u>					
M317	M	26.1	7.3	8.2	4.06
M320	M	29.3	7.7	8.3	3.96
<u>130d</u>					
M319	F	306.8	16.7	18.0	38.55
M331	F	325.0	17.7	17.9	39.89
<u>150d</u>					
M349	F	-	-	-	-

Table II

The Distribution of Mu Opioid Receptor Binding Sites in
Day 70 and Day 150 Fetal Monkeys

Area	70 day (nCi/g) (n=3)	150 day (nCi/g) (n=1)
TELENCEPHALON		
Septum	218.8 ± 95.8	760
Amygdala	1170.1 ± 364.8	2604
Caudate	519.7 ± 186.9	
Putamen	269.8 ± 26.3	
Caudate/Putamen		833.4
Patch		1316.5
Matrix		943.3
Globus Pallidus (GP)	856.6 ± 364.8	
GP external		1418.3
GP internal		236.5
DIENCEPHALON		
<u>Thalamus</u>		
Mediodorsal	5548.9 ± 384.6	4074.0
Paraventricular	2243.5 ± 182.9	6674.2
Laterodorsal		5935.2
Ventrolateral	2961.1 ± 172.5	4072.3
Reticular	4597.8 ± 910.7	4548.7
Medial Geniculate	1952.5 ± 59.4	
Dorsomedial		3478.0
Ventromedial		4428.2
Arcuate	1574.9 ± 157.5	3801.7
MESENCEPHALON		
Fasciculus Retroflexus	2663.8 ± 169.6	3130.1
Periaqueductal Grey	1021.3 ± 159.8	1016.8
Superior Colliculus	1400.4 ± 163.8	1199.9
Reticular Formation	1072.7 ± 73.9	2159.4
METENCEPHALON		
Pontine Raphe Nucleus	1298.9 ± 101.4	
Pontine Reticular Nucleus	1480.2 ± 207.9	3698.4
Spinal Trigeminal Nucleus		2387.9
Motor	1188.7 ± 282.9	
Sensory	1284.3 ± 304.2	
Inferior Olive	2546.3 ± 164.9	1497.8

Table III.
Localization of mu receptor binding and mRNA in 70 day fetal rhesus monkey.

Telencephalon	Mu receptor Binding	Mu receptor mRNA
Cortex		
Frontal	+	-
Parietal	-	-
Temporal	-	-
Cingulate	+	-
Piriform	+	-
Occipital	-	-
Olfactory Bulb	+	+++
Olfactory Tubercle	+	-
Septum	+	++
Diagonal Band of Broca	+	++
Nucleus Accumbens	+	++
Caudate	+	+
Putamen	+	++
Globus Pallidus	+	-
Amygdala	++	+++
Hippocampus	+	++

Diencephalon

Thalamus

Anteromedial	++++	+++
Paraventricular	+++	++
Laterodorsal	++++	++
Mediodorsal		++
Centromedial	++++	++
Centrolateral	++++	+++
Reticular	++++	++/+++
Ventrolateral	+++	+++
Medial Geniculate	++	

Habenula

Medial	++++	+++
Lateral	-	-

Hypothalamus

Medial Preoptic Area	+	-
Lateral Preoptic Area	+	-
Supraoptic Nucleus	++	+
Arcuate	++	+
Paraventricular	+	+
Dorsomedial	++	+
Lateral Hypothalamus	++	+
Mammillary Nuclei	++	-

Mesencephalon

Substantia Nigra	++	+
Ventral Tegmental Area	++	+
Periaqueductal Grey	++	
Superior Colliculus	++	+
Inferior Colliculus	++	+
Reticular Formation	++	+
Fasciculus Retroflexus	+++	

Metencephalon/Myelencephalon

Dorsal Raphe	+	
Parabrachial Nucleus	++	+
Dorsal Tegmental Nucleus	++	-
Locus Coeruleus	+	-
Pontine Raphe Nucleus	++	+
Pontine Reticular Nucleus	++	+
Spinal Trigeminal Nucleus	++	++/+++
Cerebellum		
Cortex	+	-
Deep Nuclei	+	+
Vermis	-	-
Medulla		
Ambiguous Nucleus		+++
Nucleus Tractus Solitarius		++
Spinal Trigeminal Nucleus		+++
Lateral Lemniscus		++

++++ = very dense (BD: >3000 nCi/g)
+++ = dense (BD: 2000-3000 nCi/g)
++ = moderate (BD: 1000-2000 nCi/g)
+ = low (BD: 0-1000 nCi/g)
- = zero
blank = no data available

Table IV. Quantification of cell numbers within the fetal thalamus and epithalamus at various developmental stages.

Animals	Total number of cells	Cells with grains	Percentage
40 day			
Ventral Thalamus	284	154	54%
60 day			
Habenula	306	89	29%
Reticular Nucleus	183	68	37%
70 day			
Habenula	164	110	67%
Reticular Nucleus	119	93	78%
Centromedian Nucleus	163	88	54%
130 day			
Habenula	120	83	69%
Laterodorsal Nucleus	32	17	53%
Paraventricular Nucleus	40	17	43%

The total number of cells and the number of cells containing autoradiographic grains were counted within a $155 \mu\text{m}^2$ of thalamic nuclei and the habenula. From this, the percentage of cells containing autoradiographic grains was estimated.